University of Tennessee, Knoxville
TRACE: Tennessee Research and Creative Exchange

Doctoral Dissertations | Graduate School

12-1952

Heat Transfer to Liquid Metals in a Thermal Entrance Region

William B. Harrison
University of Tennessee - Knoxville

Follow this and additional works at: https://trace.tennessee.edu/utk_graddiss

 Part of the Chemical Engineering Commons

Recommended Citation

Harrison, William B., "Heat Transfer to Liquid Metals in a Thermal Entrance Region. " PhD diss., University of Tennessee, 1952.
https://trace.tennessee.edu/utk_graddiss/1491

This Dissertation is brought to you for free and open access by the Graduate School at TRACE: Tennessee Research and Creative Exchange. It has been accepted for inclusion in Doctoral Dissertations by an authorized administrator of TRACE: Tennessee Research and Creative Exchange. For more information, please contact trace@utk.edu.

To the Graduate Council:

I am submitting herewith a dissertation written by William B. Harrison entitled "Heat Transfer to Liquid Metals in a Thermal Entrance Region." I have examined the final electronic copy of this dissertation for form and content and recommend that it be accepted in partial fulfillment of the requirements for the degree of Doctor of Philosophy, with a major in Chemical Engineering.

R. M. Boarts, Major Professor

We have read this dissertation and recommend its acceptance:

H. J. Garber, H. F. Johnson, S. H. Jury, R. L. Wilson

Accepted for the Council:

Carolyn R. Hodges

Vice Provost and Dean of the Graduate School

(Original signatures are on file with official student records.)

December 1, 1952

To the Graduate Council:

I am submitting herewith a thesis written by William B. Harrison entitled "Heat Transfer to Liquid Metals in a Thermal Entrance Region." I recommend that it be accepted in partial fulfillment of the requirements for the degree of Doctor of Philosophy, with a major in Chemical Engineering.

Major Professor

We have read this thesis
and recommend its acceptance:

Accepted for the Council:

Dean of the Graduate School

HEAT TRANSFER TO LIQUID METALS IN A THERMAL ENTRANCE REGION

33

A THESIS

Submitted to
The Graduate Council
of
The University of Tennessee
in
Partial Fulfillment of the Requirements
for the degree of
Doctor of Philosophy

---

by

William B. Harrison

December 1952

ACKNOWLEDGMENT

The work described in the following report was financed by and performed at the Oak Ridge National Laboratory. The administrative details of this arrangement were prescribed by Dr. A. M. Weinberg, Dr. C. E. Winters, and Dr. R. N. Lyon and technical supervision of the work was performed by Dr. H. F. Poppendiek. Financial support was given to the project by the ANP Division which is directed by Dr. R. C. Briant. The role of each of these men in making this work possible is gratefully acknowledged.

The Graduate Committee members at the University of Tennessee were Dr. R. M. Boarts, Professor H. J. Garber, Dr. H. F. Johnson, Dr. S. H. Jury, and Dr. R. L. Wilson. The members at Oak Ridge were Dr. R. N. Lyon and Dr. H. F. Poppendiek. Collectively, these men offered many stimulating ideas and much good advice. Their cooperation in attending committee meetings is also noted with appreciation.

Another source for stimulating ideas and good advice was the group of men who were also working at ORNL on related heat transfer problems. Specifically, Mr. H. C. Claiborne, Mr. W. S. Farmer, Dr. H. W. Hoffman, Mr. N. F. Lansing and Mr. Malcolm Richardson contributed to the project in various ways. Special thanks are extended to Dr. D. C. Hamilton in this same connection.

For the many craft services the project received, Mr. C. G. Hubbard and his men are particularly thanked for their part in bringing the project to completion.

305514

Thanks are also extended to Mr. J. J. Droher and Dr. E. E. Stansbury of the University of Tennessee for the use of their equipment in the wetting experiments.

Miss T. K. Sutton performed the typing in this report and Mrs. Jo Millsaps prepared the figures. The excellent work performed by these ladies is greatly appreciated.

In retrospect, there are three people without whom the project would not have been completed, and possibly it would never have been started. They are Dr. R. M. Boarts, who motivated the inspiration and desire to pursue this work; Dr. H. F. Poppendiek, who eased the project over many hurdles at the plant by his helpful suggestions and moral support; and my wife, Josephine, who eased the project over many hurdles at home by her cooperation and understanding. To her, this work is dedicated.

W B Harrison

W. B. Harrison

SUMMARY

The purpose of the present work is to explore analytically and experimentally the heat transfer to liquid metals in turbulent flow within the thermal entrance region of circular tubes having uniform wall temperature. Since liquid metals are characterized by high thermal conductivity, emphasis has been placed on analytical conduction solutions which neglect the contribution to heat transfer that is made by the eddy motion of a fluid in turbulent flow. Three solutions, which differ only in the postulated velocity distribution of the fluid, have been selected for comparison. The postulated velocity distributions are: (1) uniform, (2) parabolic and, (3) velocity proportional to distance from the channel wall raised to the one-seventh power. The third distribution is usually referred to as the one-seventh power law distribution. Other related entrance region solutions are briefly surveyed.

In view of the important role played by the molecular thermal conductivity in heat transfer to liquid metals in a direction normal to a tube wall, the influence of thermal conductivity on heat transfer parallel to a tube wall has been examined. A comparison has been made between conduction solutions for the case of a fluid with uniform velocity for two systems of differing boundary conditions in which the longitudinal conduction term is included, and an analogous system in which the longitudinal conduction term has been neglected.

It was concluded that the effect of longitudinal conduction may be neglected in cases of heat transfer to liquid metals in turbulent flow.

Experimental work performed in connection with this study consisted of taking heat transfer data to mercury and sodium in tubes of 1/16 inch and 1/8 inch length in combination with diameters of 1/16 inch and 1/8 inch. The mercury heat transfer data for three different test sections compare favorably with the conduction solution for a postulated velocity distribution according to the one-seventh power law. These data were taken over a range of Reynolds modulus from 20,000 to 200,000 and heat transfer coefficients up to 66,300 Btu/hr.ft.^{2} $^\circ$F. were achieved. The experimental data were higher than the predictions at the high range of Reynolds numbers, presumably because the predictions neglected the contribution of the eddy conduction to the heat transfer mechanism.

Sodium data were erratic and low when compared with the mercury data or the conduction solutions. In an effort to explain this observation, it has been shown that, if a non-wetted condition existed, the small test section diameter and the high thermal conductivity of sodium would combine to maximize the effects on the heat transfer. An attempt was made to corroborate the hypothesis of non-wetting with an experimental study of interfacial electrical resistance but the results were inconclusive.

Recommendations are made for extending the range of experimental operation to low Reynolds modulus (1000), so as to investigate the influence of the velocity distribution, and to high Reynolds modulus (greater than 200,000) to study the influence of eddy conduction.

The test section which was designed for the present studies can be easily adapted for use with other fluids or for other entrance conditions. Since it does tend to maximize effects of non-wetting, the present test section may be useful in pursuing thermal studies of wetting effects.

The implication is clear that heat transfer coefficients greater than 500,000 Btu/hr. ft.^{2} $^\circ$F. should be attainable with sodium if the difficulties encountered in the present work can be overcome.

TABLE OF CONTENTS

CHAPTER PAGE

LIST OF TABLES

LIST OF FIGURES

FIGURE PAGE

CHAPTER I

INTRODUCTION

In many practical heat transfer systems, there persists the challenge to transfer large quantities of heat through small areas. In recent years, workers in the heat transfer field have become increasingly aware that liquid metals offer unique possibilities for meeting this challenge.

The existing studies which demonstrate the advantages of liquid metals over other heat transfer media are based on comparisons of heat transfer in long channels in which entrance effects are considered to be negligible. In the present work, it is shown that entrance effects in short tubes can be utilized so as to yield even higher values of heat transfer coefficients or heat flux to liquid metals than are obtained in long tubes.

Since the terms "entrance effects", "short" tubes, "long" tubes, and, in fact, "heat transfer in a thermal entrance region", depend on several related concepts in the fields of heat transfer and fluid mechanics, the present chapter is devoted to a discussion of some of these concepts which pertain to the present study. Though most of the discussion is applicable to all fluids, special attention is devoted to liquid metals.

Liquid Metals as Heat Transfer Media

The liquid metals of most interest for transferring heat are characterized by the following properties:

1. Moderate melting point
2. High boiling point
3. Moderate viscosity
4. High thermal conductivity

In order to illustrate these characteristic properties, a few representative examples are shown in Table I for comparison. Practical application of these characteristics of liquid metals to heat exchange problems would indicate (a) operation of heat exchangers at high temperatures without the requirement of high pressure which is attendant with the use of more common heat transfer media, and (b) higher attainable heat transfer coefficients and heat fluxes than can be attained with common heat transfer media for a given pumping power.

Boundary Layer Development

In liquid metals, as in more common fluids, the heat transfer conditions in an entrance region are quite different from the conditions which prevail far downstream from the entrance. In order to illustrate this point, consider the velocity distribution of a fluid initially at uniform velocity and temperature as it enters a closed channel and assume that no heat transfer occurs. The portion of the fluid adjacent to the channel wall is slowed to zero velocity. Shear (internal friction) forces within the fluid spread the drag influence of the portion near the channel wall, while the fluid near the center of the channel may still have essentially a uniform velocity. The region of fluid in which the velocity distribution has been greatly influenced by the presence of the interface at zero velocity is known

TABLE I

A COMPARISON OF TYPICAL PHYSICAL PROPERTIES OF LIQUID HEAT TRANSFER DATA

Liquid	m.p., °F.	b.p., °F.	μ, Absolute Viscosity $\frac{lb.}{ft.hr.}$	°F.	k, Thermal Conductivity $\frac{Btu}{hr.ft.^oF}$	°F	c, Heat Capacity $\frac{Btu}{lb.^oF}$	°F	Prandtl Modulus $\frac{c\mu}{k}$	°F
mercury (15,24)*	-38	675	3.71	70	5.05	70	0.033	70	0.0245	70
			2.87	230	6.20	230	0.033	230	0.0152	230
sodium (24)	208	1621	1.7	212	49.9	212	0.33	212	0.011	212
			1.1	392	46.7	392	0.32	392	0.0075	392
sodium-potassium alloy (22% Na, 78% K by wt.) (24)	12	1443	1.15	212	14.1	212	0.23	212	0.019	212
			0.79	392	14.6	392	0.23	392	0.012	392
lead-bismuth alloy (44.5% Pb, 55.5% Bi by wt.)(24)	257	3038	4.3		6.35	581	0.035	581	0.024	581
water (26)	32	212	2.36	70	0.34	70	1.00	70	6.85	70
			0.70	210	0.41	210	1.00	212	1.69	210
light oil (26)			7.75	212	0.075	212				
Dowtherm A(73.5% diphenyl oxide, 26.5% diphenyl)(7)	54	496	2.42	496	.105	496	0.63	496		

* Numbers in parenthesis refer to Bibliography.

as the boundary layer. The growth of this boundary layer from zero thickness (at the entrance) until it encompasses the entire channel is called "hydrodynamic" boundary layer development. Thus, a completely developed hydrodynamic boundary layer signifies a fully established flow regime, or velocity distribution. The distance (from the entrance) required for this complete development to take place is often referred to as "hydrodynamic entry length."

In a manner similar to hydrodynamic boundary layer development, a fluid of uniform temperature undergoes "thermal" boundary layer development as it enters a heated channel. That is, the fluid in contact with the channel wall must assume the temperature of the wall. The influence of this region near the wall is then spread toward the center of the channel in a manner analogous to the growth of the hydrodynamic boundary layer. The distance required for the temperature distribution to become established is called the "thermal entry length."

For the case of hydrodynamic boundary layer development, the flow regime may be completely laminar in nature, or initially laminar and then turbulent. The magnitude of the Reynolds modulus, $\frac{DU\rho}{\mu}$, and the geometry of the flow path upstream from the entrance determine the character of the flow regime in an isothermal stream. In a non-isothermal stream, the velocity distribution is influenced by the variation of physical properties of the fluid with temperature. All of these factors have an influence on the hydrodynamic entry length, but the chief influence is that entry length increases with Reynolds modulus. In the case of thermal boundary layer development, the thermal

effects are imposed on whatever flow regime is coexistent. Thus, the Reynolds modulus and upstream conduit geometry influence thermal boundary layer development by their effects on the flow regime.

Although the case of simultaneous hydrodynamic and thermal boundary layer development is of much interest, the present study is restricted to systems in which the hydrodynamic regime or velocity distribution is well established and only a thermal boundary layer development is occurring. Such a system is illustrated by a fluid flowing in a tube, of which an upstream section is adiabatic and a downstream section is heated. If the adiabatic section is sufficiently long that velocity distribution is established at the beginning of the heated section, thermal boundary layer development occurs in the heated section. The beginning of the heated section is then a "thermal entrance region." The beginning of the adiabatic section would be a "hydrodynamic entrance region". In each case the entry length is the length of channel required to contain the entrance region. These concepts may be used to define a "long" tube as one in which the temperature and velocity distributions are established and in which the effects of an entrance region are negligible. A "short" tube is one in which the boundary layer development is occurring or in which the effects of boundary layer development are noticeable. The so-called "entrance effects" are then the results of hydrodynamic or thermal boundary layer development in an entrance region.

The Infinite Heat Transfer Coefficient

One reason for giving attention to the entrance region is that heat transfer coefficients can reach extremely high values at the beginning of a heated section. In certain ideal cases which are discussed later, the heat transfer coefficient approaches an infinite value when the heated section approaches zero length, and it drops rapidly toward the lower values characterized by well-established velocity and temperature profiles as the length increases. This may be seen more clearly by considering the definition of heat transfer coefficient as the term is currently used.

Let $\frac{q}{A}$[1] be the heat flux (Btu/hr. ft^2.) across a fluid-solid interface, where q is the heat rate (Btu/hr.) and A is the heat transfer surface area (ft^2). The fluid adjacent to the wall must be in laminar motion, and the heat transfer through the fluid is by molecular conduction only. Hence, the following equation may be written for variation of the heat flux at the channel wall with distance x from the entrance of the heated section:

$$\left(\frac{q}{A}\right)_x = h_x(t_w - t_m) = -k\frac{\partial t}{\partial y}(x,0) \qquad \text{I-1.}$$

In this equation, k represents the molecular thermal conductivity. Temperature is represented by t, and t_w and t_m refer to the wall temperature and mixed mean fluid temperature, respectively. The variable x is

---

1. See Appendix H for Nomenclature

measured along the axis of the channel, with x = 0 at the beginning of the heated section, while y is the distance from the channel wall to a point in the fluid. The subscript x is used to denote that $\frac{q}{A}$, h, and $(t_w - t_m)$ are the functions of distance from the beginning of the heated section. The manner of writing the temperature gradient in the partial derivative notation is used to denote that $\frac{\partial t}{\partial y}$ is a function of x and y and that $\frac{\partial t}{\partial y}$ as used in the Equation I-1 is evaluated at y = 0 (the fluid-solid interface). Equation I-1 may be used to define the heat transfer coefficient as follows:

$$h_x = \frac{-k \frac{\partial t}{\partial y}(x,0)}{(t_w - t_m)} \qquad \text{I-2}$$

There are two ideal cases which may be considered to illustrate the point that at the entrance of the heat transfer region the heat transfer coefficient is infinite. If a fluid of uniform temperature is flowing in a conduit of the same temperature, and the wall temperature at x = 0 is raised to a new value which prevails for all positive values of x, it can be shown that $\frac{\partial t}{\partial y}(x,0)$ approaches an infinite value as x approaches zero. Meanwhile, the value of $(t_w - t_m)$ at x = 0 is fixed at a finite value. The other case is one of a heat flux discontinuity instead of a temperature discontinuity at x = 0. If a fluid of uniform temperature is flowing in a conduit of the same temperature, and a uniform wall heat flux is applied at x = 0 and prevails for all positive values of x, it can be shown that $\frac{\partial t}{\partial y}(x,0)$ is finite while $(t_w - t_m)$ approaches zero as x approaches zero. In both cases, it is seen that the heat transfer coefficient must approach an infinite value as x

approaches zero. In the present study, thermal entrance regions of uniform wall temperature are of principal interest.

The Turbulent Flow Regime

As pointed out previously, the thermal effects during thermal boundary layer development are imposed on whatever flow regime is coexistent. In the present study, the flow regime is assumed to be turbulent.

The velocity distribution within a fluid in turbulent flow is often represented by a power law as derived by Prandtl (32). The power law most commonly utilized to describe velocity distribution up to Reynolds modulus of 50,000 is of the form $u = B\left(\frac{y}{b}\right)^{1/7}$, where u is fluid velocity at a distance y from the wall of a channel of radius b. The maximum velocity is represented approximately by the constant B. Schlichting (35) considers this one-seventh power law to be suitable for Reynolds modulus up to 100,000. For higher values of Reynolds modulus, the derivation of Prandtl is altered somewhat to give a one-eight power law for velocity at Re = 200,000 and a one-tenth power law for velocity at $Re = 2 \times 10^6$. Two limiting distributions for velocity may also be considered: (1) uniform velocity distribution, and (2) parabolic velocity distribution. As Reynolds modulus is increased to higher and higher values, the velocity distribution across the turbulent core becomes increasingly uniform. In the limit, one may conceive of a completely uniform velocity throughout the conduit. The other limiting velocity distribution is the parabolic distribution which is

characteristic of laminar flow at Reynolds moduli up to 2000-4000. Clearly, the turbulent flow regime cannot attain either of these limiting velocity distributions but they may be used to illustrate the influence of velocity distribution on the analytical heat transfer solutions.

The well-established turbulent flow regime within a closed channel is considered to have three different regions of flow: (1) the laminar sublayer, (2) the buffer region, and (3) the turbulent core. The laminar sublayer comprises the band adjacent to the channel wall, where the fluid is in laminar motion. Heat is transferred across it by molecular conduction only, as mentioned in the discussion of the definition of heat transfer coefficient. The buffer layer which lies between the laminar sublayer and the turbulent core is a zone in which eddies begin to occur, and the turbulent core is a region which is characterized by pronounced eddy motion.

The Role of Molecular Conduction in Heat Transfer to Liquid Metals

Within the turbulent core of a fluid, heat is transferred by combined molecular and eddy conduction. In ordinary fluids, the molecular conduction is small compared with the eddy conduction and it may be neglected in the analytical heat transfer computations for the core zone. In liquid metals, however, this is not the case. As a result of their high thermal conductivity, it is necessary to retain the molecular conduction contribution in considering the core analysis as well as in the analysis of the buffer layer and the laminar sublayer.

It was the inclusion of the molecular conduction term in the turbulent core analysis which distinguished the pioneer theoretical work of Martinelli (27) and Lyon (25) on heat transfer to liquid metals in regions of established temperature and velocity distribution. In the analytical solutions which are discussed in greatest detail in the present report, this line of reasoning is extended one step further. The solutions are based on the postulate that the eddy conduction contribution is negligible compared with that of the molecular conduction. The magnitude of the eddy conduction contribution is a function of Reynolds modulus, increasing as the modulus increases. One implication of the postulate may be that the Reynolds modulus is sufficiently low that the eddy conduction contribution is negligible. Another consideration is that in regions very near to the beginning of the heated section of a channel, the thermal boundary layer does not extend far beyond the laminar sublayer or the buffer layer, and the extent of turbulence in the core has little influence on the total conduction in the region of importance. These two thoughts are closely related by the fact that the thickness of the laminar sublayer or the buffer layer decreases as the Reynolds modulus increases. Additional discussion of these concepts will be presented later.

Purpose and Scope

It is the purpose of the present work to examine both analytically and experimentally the mechanism of heat transfer to liquid metals in a thermal entrance region. The scope of the work is confined

to the turbulent flow regime, the circular tube geometry, and the thermal entrance region of uniform wall temperature. The treatment of the subject includes a review of the existing analytical solutions and experimental data for heat transfer in entrance regions; a detailed examination of one of the basic postulates which is common to all of these solutions; a description of two systems which were designed and operated in order to obtain pertinent experimental data; and a discussion of the experimental data in comparison with the analytical predictions.

The analytical solutions are discussed in Chapter II with respect to the different postulates on which they are based and the resulting differences which arise in the heat transfer predictions.

The postulate which is examined in detail is that the amount of heat conducted in an axial direction is negligible compared with the amount conducted in a radial direction at any position within the fluid. This postulate is examined in Chapter III in order to determine whether or not it is applicable to fluids of high thermal conductivity.

Heat transfer data to mercury and to sodium were taken in the same type of test section, but the overall systems differed. These experimental systems and their operation are described in Chapter IV.

The experimental data for entrance region heat transfer to mercury and sodium are summarized in Chapter V, and comparison is made between experimental results and the analytical predictions. The heat transfer data to sodium indicate the need for investigation of contact resistance between copper and sodium, which is discussed in Chapter VI as a means of explaining the sodium data.

In Chapter VII, an effort is made to summarize the conclusions and recommendations which may be drawn from the present work.

In the Appendix, several pertinent discussions are presented in order to amplify material in the body of the report or to examine features of the experimental systems. Symbols used in the text and their definitions are tabulated in the last section of the Appendix.

CHAPTER II

ANALYTICAL SOLUTIONS FOR HEAT TRANSFER IN THE ENTRANCE REGION

A solution of the temperature field within a moving fluid may be used to compute the local heat transfer coefficient as defined in Equation I-2 or the local Nusselt modulus, Nu_x, which comes directly from Equation I-2, as follows:

$$Nu_x = \frac{h_x D}{k} = \frac{-D \frac{\partial t}{\partial y}(x,0)}{(t_w - t_m)_x} \qquad \text{II-1}$$

It is possible to obtain approximate solutions for Nu_x for many real systems by developing solutions for related ideal systems, or models. As a result of the important role of the high molecular conduction in heat transfer to liquid metals, the possibility exists that solutions based on molecular conduction alone may serve as suitable approximations for systems involving liquid metal streams at low or moderate Reynolds modulus, where the eddy contribution to the heat transfer may be small compared with the molecular conduction. It is significant to view a few of these solutions for comparison with each other and then see how experimental observations are related to them.

Conduction Solutions

The Fourier-Poisson equation may be used to describe the temperature field arising from heat transfer by molecular conduction within a moving fluid.[1] In rectangular coordinates this is written as follows:

---

1. See reference (8).

$$c\rho\left[\frac{\partial t}{\partial \theta}+u_x\frac{\partial t}{\partial x}+u_y\frac{\partial t}{\partial y}+u_z\frac{\partial t}{\partial z}\right]=\frac{\partial}{\partial x}\left[k\frac{\partial t}{\partial x}\right]+\frac{\partial}{\partial y}\left[k\frac{\partial t}{\partial y}\right]+\frac{\partial}{\partial z}\left[k\frac{\partial t}{\partial z}\right] \qquad \text{II-2}$$

where c is heat capacity, ρ is density, t is temperature, θ is time, and u_x, u_y, and u_z are velocity components parallel to the coordinate axes x, y, and z, respectively.

In cylindrical coordinates, it is:

$$c\rho\left[\frac{\partial t}{\partial \theta}+u_x\frac{\partial t}{\partial x}+u_r\frac{\partial t}{\partial r}+\frac{u_\phi}{r}\frac{\partial t}{\partial \phi}\right]=\frac{k}{r}\frac{\partial t}{\partial r}+\frac{\partial}{\partial x}\left[k\frac{\partial t}{\partial x}\right]+\frac{\partial}{\partial r}\left[k\frac{\partial t}{\partial r}\right]+\frac{1}{r^2}\frac{\partial}{\partial \phi}\left[k\frac{\partial t}{\partial \phi}\right] \qquad \text{II-3}$$

where r is radial distance from the x axis, and Φ is angular displacement. Several postulates may be made in order to define the ideal system:

1. Conduction is negligible parallel to the direction of flow; i.e., $k\frac{\partial t}{\partial x}=0$
2. The temperature field is symmetrical about the x axis; i.e., $\frac{\partial t}{\partial \Phi}=0$
3. Steady conditions prevail with respect to time; i.e., $\frac{\partial t}{\partial \theta}=0$.
4. The velocity distribution is established; i.e., $u_r=u_\phi=0$
5. Physical properties are uniform and independent of temperature; i.e, $\frac{\partial}{\partial x}\left[k\frac{\partial t}{\partial x}\right]=k\frac{\partial^2 t}{\partial x^2}$

With these assumptions, the Equation II-3 becomes

$$u_x \frac{\partial t}{\partial x} = a \left[\frac{\partial^2 t}{\partial r^2} + \frac{1}{r} \frac{\partial t}{\partial r} \right] \qquad \text{II-4}$$

where r is the radial distance from the x-axis to a point in the fluid and "a" is thermal diffusivity, $\frac{k}{c\rho}$. Consider a fluid flowing through a tube of radius b. The boundary conditions postulated for the ideal heat transfer system are:

1. Initial fluid temperature is uniform; $t(0,r) = t_o$
2. Wall temperature is uniform; $t(x,b) = t_w$
3. Temperature field is axially symmetrical; $\frac{\partial t}{\partial r}(x,0) = 0$

Three analytical solutions for heat transfer in the thermal entrance region of uniform wall temperature have been selected for comparison. Each is a solution of the Fourier-Poisson equation for a special case, and each differs only in the postulated form of the velocity distribution. As pointed out in Chapter I, the turbulent velocity distribution is described by the one-seventh power law for a stream of Reynolds modulus up to about 100,000. The turbulent velocity distributions are limited to a region bounded by the uniform velocity distribution and the parabolic velocity distribution. These three velocity distributions serve to designate the analytical solutions as follows:

1. The solution presented by Graetz (13) for parabolic velocity distribution.
2. The solution presented by Graetz (14) for uniform velocity distribution.

3. The solution presented by Poppendiek (31) for velocity distribution obeying the one-seventh power law.

For the parabolic velocity distribution case, the velocity at any radius is expressed by the relation $u = 2U\left[1 - \left(\frac{r}{b}\right)^2\right]$, where U is the mean velocity. For the uniform velocity case, $u = U$; and for the one-seventh power law distribution, $u = B\left(\frac{y}{b}\right)^{1/7}$, where y is the distance from the channel wall.

Parabolic Velocity Distribution

The solution for the case of parabolic velocity distribution as developed by Graetz may be written as follows[2]:

$$Nu_x = \frac{2\left[1.499e^{-\frac{2(2.705)^2}{Pe\frac{D}{x}}} + 1.078e^{-\frac{2(6.66)^2}{Pe\frac{D}{x}}} + 0.358e^{-\frac{2(10.3)^2}{Pe\frac{D}{x}}} + \cdots\right]}{\left[0.820e^{-\frac{2(2.705)^2}{Pe\frac{D}{x}}} + 0.0972e^{-\frac{2(6.66)^2}{Pe\frac{D}{x}}} + 0.0135e^{-\frac{2(10.3)^2}{Pe\frac{D}{x}}} + \cdots\right]} \qquad \text{II-5}$$

Details of this solution are presented by Jakob (17) and Boelter et al (3). The abbreviation Pe represents the Peclet modulus, $\frac{DU\rho c}{k}$. For a region very near a thermal entrance, the solution of Graetz has not been evaluated. However, Leveque (23) presented a solution which may serve as an asymptote to augment the results of Graetz.

$$Nu_x = 1.0766\left[Pe\frac{D}{x}\right]^{\frac{1}{3}} \qquad \text{II-6}$$

---

2. See Appendix A

Equations II-5 and II-6 express the variation of local Nusselt modulus with distance x from the entrance to the heated section of a tube. It is also of interest to compare average values of Nusselt moduli over regions of distance L from the thermal entrance. The average value of Nusselt modulus may be defined as follows:

$$Nu_L = \frac{1}{L}\int_0^L Nu_x \, dx \qquad \text{II-7}$$

Thus, according to Equation II-7, average values of Nusselt modulus may be computed from solutions for local values. Equation II-5 becomes[3]

$$Nu_L = \frac{1}{4} Pe \frac{D}{L} \ln \frac{1}{\left[0.820 e^{-\frac{2(2.705)^2}{Pe\frac{D}{L}}} + 0.0972 e^{-\frac{2(6.66)^2}{Pe\frac{D}{L}}} + 0.0135 e^{-\frac{2(10.3)^2}{Pe\frac{D}{L}}} + \cdots\right]} \qquad \text{II-8}$$

and Equation II-6 becomes

$$Nu_L = 1.615 \left[Pe \frac{D}{L}\right]^{\frac{1}{3}} \qquad \text{II-9}$$

---

3. See Appendix A

Uniform Velocity Distribution

For the uniform velocity case, the local Nusselt modulus is

$$Nu_x = \frac{\sum_{n=1}^{\infty} e^{-\frac{4\alpha_n^2}{Pe\frac{D}{x}}}}{\sum_{n=1}^{\infty} \frac{1}{\alpha_n^2} e^{-\frac{4\alpha_n^2}{Pe\frac{D}{x}}}} \qquad \text{II-10}$$

where α_n are roots of $J_o(\alpha) = 0$

Average values of Nusselt modulus for the case of uniform velocity are obtained from Equation II-10, which gives[4]

$$Nu_L = \frac{1}{4} Pe \frac{D}{L} \ln \frac{1}{\sum_{n=1}^{\infty} \frac{1}{\alpha_n^2} e^{-\frac{4\alpha_n^2}{Pe\frac{D}{L}}}} \qquad \text{II-11}$$

Equation II-10 and II-11 may be augmented by an asymptotic solution presented by Poppendiek (31), in a form analogous to the Leveque solution which is mentioned above (Equation II-6).

$$Nu_x = \frac{1}{\Gamma\left(\frac{1}{m+2}+1\right)} \left[\frac{m+1}{2^{1-m}(m+2)} Pe \frac{D}{x}\right]^{\frac{1}{m+2}} \qquad \text{II-12}$$

In this solution, the m is defined by the power law velocity distribution, $u = B\left(\frac{y}{b}\right)^m$. For the case of uniform velocity, $m = 0$ and $B = U$. Hence, Equation II-12 may be written as follows:

$$Nu_x = 0.564 \left[Pe \frac{D}{x}\right]^{\frac{1}{2}} \qquad \text{II-13}$$

---

4. See Appendix B

or

$$Nu_L = 1.128 \left[Pe \frac{D}{L}\right]^{\frac{1}{2}} \qquad \text{II-14}$$

One-seventh Power Law Velocity Distribution

Poppendiek (30) presented a conduction solution for a fluid with velocity obeying the one-seventh power law within a conduit formed by two parallel plates. The boundary conditions were the same as those listed previously: uniform initial fluid temperature, uniform wall temperature, and axial symmetry.

By altering the solution slightly, it can be used as an approximation for the analogous circular tube system. However, the approximation is good only for large values (greater than 1000) of the modulus, $Pe \frac{D}{x}$. The asymtotic solution which Poppendiek (31) later presented is also applicable over the high region of $Pe \frac{D}{x}$ and it is much easier to use for computations. Thus, for the case in which velocity distribution obeys the one-seventh power law, $u = B \left(\frac{y}{b}\right)^{1/7}$, Equation II-12 may be written as follows:

$$Nu_x = 0.638 \left[Pe \frac{D}{x}\right]^{\frac{7}{15}} \qquad \text{II-15}$$

and

$$Nu_L = 1.196 \left[Pe \frac{D}{L}\right]^{\frac{7}{15}} \qquad \text{II-16}$$

Comparison of Solutions

Note that all solutions described above are for the same system with the same boundary conditions. In all cases, heat is transferred

radially by molecular conduction only (as distinguished from eddy conduction), and longitudinal or axial conduction is neglected. The only primary difference between them is the postulated velocity distribution. Comparison of values of local Nusselt moduli computed from these solutions is shown graphically on Figure 1. Computed values for the one-seventh power law are extrapolated in accordance with the relationship between the three analogous solutions for conduits bounded by parallel plates. Also shown on Figure 1 are values taken from the analytical results of Seban and Shimazaki (37) for fluids of high thermal conductivity in a thermal entrance region of uniform wall temperature. Their computations were based upon a differential equation similar to Equation II-4 but including the eddy conduction contribution as follows:

$$u \frac{\partial t}{\partial x} = \frac{1}{r} \frac{\partial}{\partial r} \left[r (a + \epsilon_H) \frac{\partial t}{\partial r} \right] \qquad \text{II-17}$$

where "ϵ_H" is eddy diffusivity of heat and "a" is thermal diffusivity. Equation II-17 reduces to Equation II-4 if "ϵ_H" is negligible compared with "a", and "a" is assumed to be constant. Numerical integrations were performed for the cases studied, which were characterized by two Reynolds moduli, 10^4 and 10^5, with Prandtl modulus[5] of 0.01. Although there is some uncertainty regarding their results because of large radial increments used in the integrations, the values shown on

---

5. Note: $Pr = \frac{c \mu}{k}$; $Pe = Re \cdot Pr$

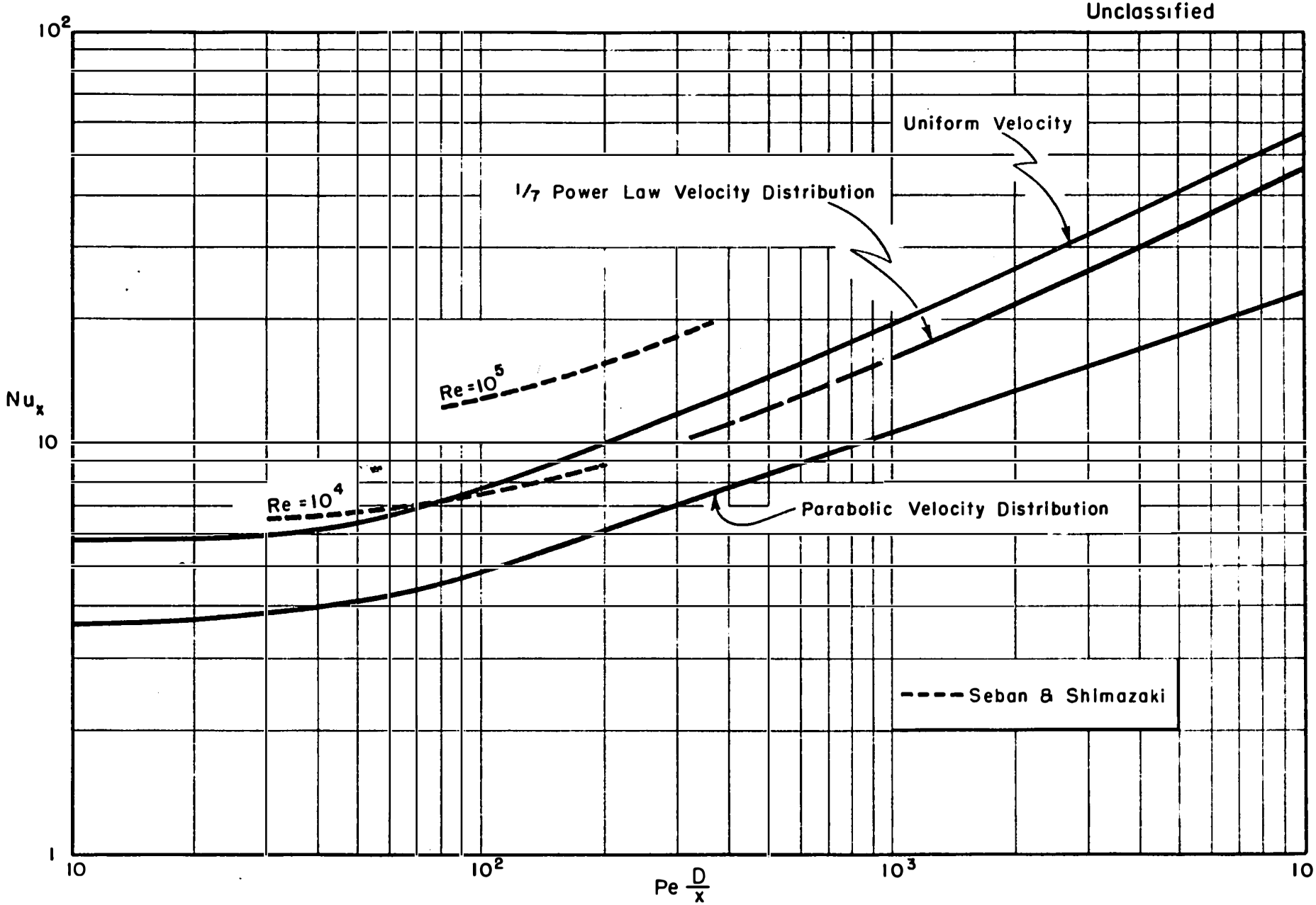

Fig. 1. Local Nusselt Moduli in a Thermal Entrance Region of Uniform Wall Temperature

Figure 1 are easily extrapolated to the predicted values for heat transfer to liquid metals in long tubes, according to another equation presented by Seban and Shimazaki (36):

$$Nu = 5.0 + 0.025 \left[Pe\right]^{0.8} \qquad \text{II-18}$$

As in the studies made by Martinelli (27) and Lyon (25), this equation developed by Seban and Shimazaki is based on the analogy between momentum and heat transfer in high-conductivity fluids of established velocity and temperature distributions. One may consider that the curve for Re = 10^4 and Pr = 0.01, as extrapolated to the long tube value, is typical of the many possible combinations of Reynolds modulus and Prandtl modulus. That is, for a given Peclet modulus, Equation II-18 defines the Nusselt modulus at which the curve levels off for large values of x, and the conduction solution serves as a bound for the Nusselt modulus at very small values of x. The point at which any case may be adequately represented by the conduction solution depends on the magnitude of the Reynolds modulus and the thickness of the thermal boundary layer as mentioned in Chapter I. The solutions for average values of Nusselt moduli are shown on Figure 2. It is with these solutions that the present experimental data will be compared in Chapter V. Several other investigations of heat transfer in entrance regions have been made, but they are not applicable to the present study. A few of these may be noted briefly.

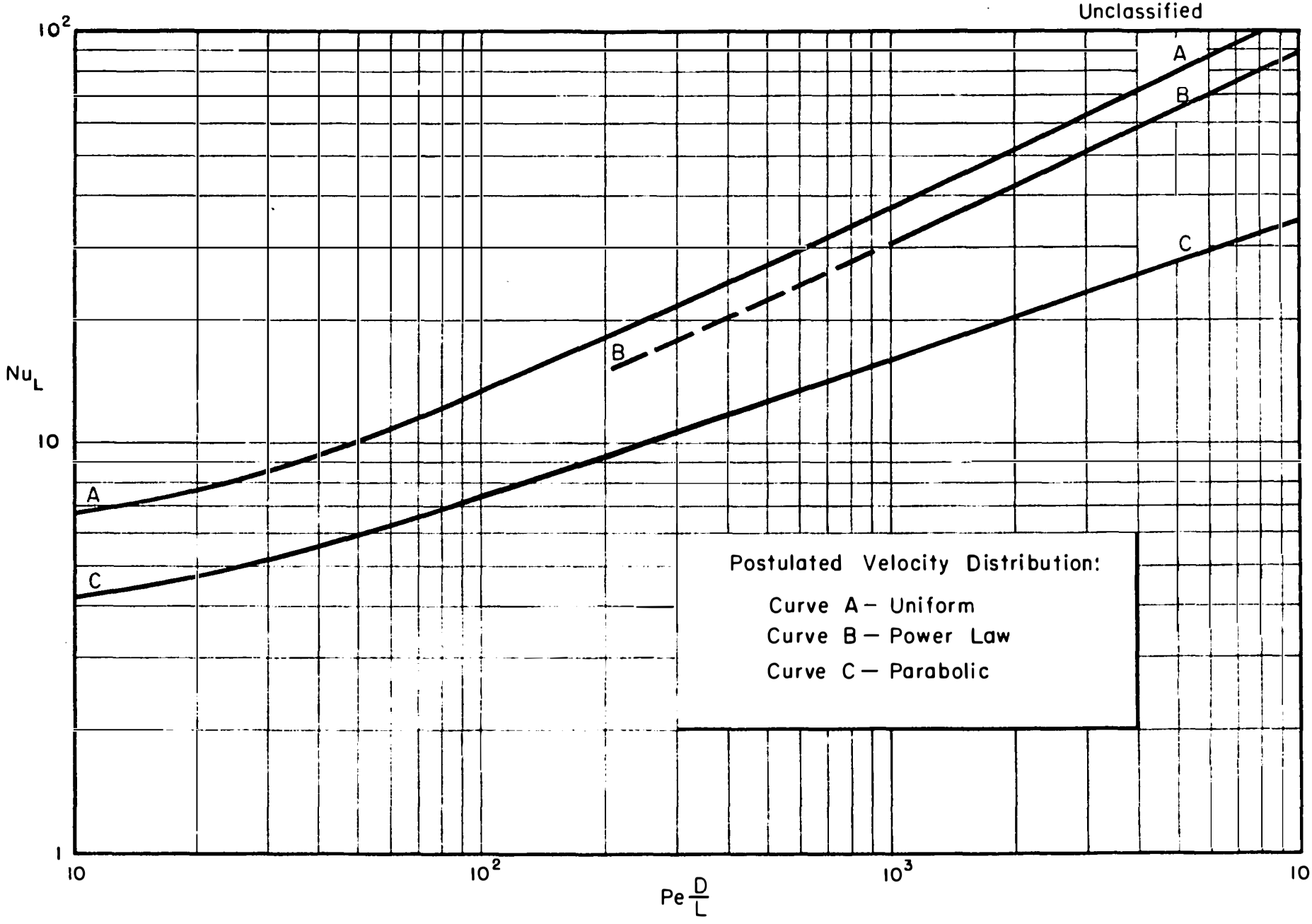

Fig. 2. Average Nusselt Moduli in a Thermal Entrance Region of Uniform Wall Temperature

Related Analytical Investigations

The work of Latzko (21) is of considerable historic interest but it may not be applied to systems involving liquid metals because he postulated a Prandtl modulus of unity. As in the solution of Poppendiek (30) mentioned previously, Latzko also postulated that the velocity obeyed the one-seventh power law. He presented solutions for heat transfer in thermal boundary layer development, simultaneous thermal and hydrodynamic boundary layer development and intermediate cases. Part of this work has been discussed by Jakob (17).

Sanders (33) considered a general treatment of fully established temperature and velocity distributions in a pipe having a wall temperature discontinuity. As Bailey (1) has pointed out, the postulates which Sanders made are expected to be applicable only for fluids in which the major thermal resistance is near the channel wall. This implies high Prandtl modulus, eliminating applicability to liquid metals systems.

Bailey (1) set up equations representing the case of uniform velocity and temperature distributions at an entrance. Numerical integration of the energy equation was performed for Reynolds modulus of 10^5 and Pr = 0.01 up to a length of 0.1 diameter.

In all cases, it has been postulated that the longitudinal conduction is negligible. The importance of this postulate will be discussed in the next chapter.

Related Experimental Investigations

The experimental investigation discussed later in this report is unique in its scope: heat transfer to liquid metals in thermal entrance regions of uniform wall temperature. However, data are currently available for heat transfer to liquid metals in entrance regions of uniform wall flux, and to air in thermal entrance regions of uniform wall temperature. Though these investigations are not specifically related to the present discussion, they are in the same general area of entrance region heat transfer and brief descriptions of them are given below.

Johnson, Hartnett, and Clabaugh (20) presented heat transfer data to lead-bismuth eutectic in a circular tube with uniform wall heat flux. Although they were primarily interested in average heat transfer data for tubes of $L/D \cong 64$, local heat transfer coefficients were computed for $\frac{x}{D}$ of 4.6, 13.8 and 23. Reynolds modulus ranged from 7500 to 170,000; Peclet modulus from 200 to 5000; Prandtl modulus from 0.020 to 0.096; and, Nusselt modulus from 6 to 20.

English and Barrett (11) determined heat transfer coefficients to mercury in tubes having uniform wall heat flux along a heated length of about 50 diameters. Data were taken over a range of Reynolds modulus from 4000 to 45,000. Here again, the main interest of the investigation was to determine "long-tube" values of heat transfer coefficient, but the data could be used to evaluate local values for $\frac{x}{D}$ greater than about 5.

Boelter, Young, and Iversen (4) investigated local heat transfer coefficients to air in thermal entrance regions of uniform wall temperature for several different hydrodynamic entrance conditions. Their data were taken in a range of Reynolds modulus from about 17,000 to 56,000. Agreement was found between experimental results and the analytical treatment of Latzko[6] for the case of simultaneous thermal and hydrodynamic boundary layer development.

Cholette (6) determined local and average heat transfer coefficients in a tube bundle of uniform wall temperature through the range of Reynolds modulus from about 80 to 18,500. The local heat transfer coefficients reported are actually average values over length increments of about 10.5 diameters.

Humble, Lowdermilk, and Grele (16) investigated heat transfer to air with uniform wall heat flux. Poppendiek (30) used their data to estimate the variation of heat transfer coefficient with distance from the tube entrance for the Reynolds modulus of 140,000. The experimenters took data over a range of Reynolds modulus from about 5000 to 250,000.

None of the studies cited includes local or average heat transfer coefficients for regions of $\frac{x}{D}$ less than about 3 and all data for uniform heat flux cases in regions of $\frac{x}{D}$ less than 10 seem to be susceptible to large conduction errors. In contrast, the experimental test section described in Chapter IV has been used to obtain average values of heat

---

6. See page 22

transfer coefficient for $\frac{x}{D}$ as low as $\frac{1}{2}$ and it may be modified to obtain data for even smaller increments of $\frac{x}{D}$.

CHAPTER III

THE EFFECT OF LONGITUDINAL CONDUCTION IN THE THERMAL ENTRANCE REGION

In Chapter II, it was noted that all of the available solutions for heat transfer in an entrance region are based on the postulate that longitudinal conduction is negligible. Baranowski and Jury (2) are conducting a study which includes the effect of longitudinal conduction for parabolic velocity distribution within a thermal entrance region. Greatly simplified and more readily obtained solutions are achieved if uniform velocity is postulated. It is believed that, for purposes of examining the effects of longitudinal conduction in liquid metals, solutions for cases of uniform velocity will be adequate. As in solutions emphasized in Chapter II, the solutions obtained in this study are based on the postulate that heat is transferred by molecular conduction only (as distinguished from eddy conduction). Since comparisons between parallel plate systems and circular tube systems are of general interest, both geometries are considered here, although only the solutions for the circular tube systems have been evaluated. Comparisons are made of heat transfer in thermal entrance regions of uniform wall temperature for three cases of each geometry. The geometry and nomenclature are indicated on Figure 3. Odd-numbered equations are for the parallel plate geometry and the analogous equations for the circular tube geometry are even-numbered.

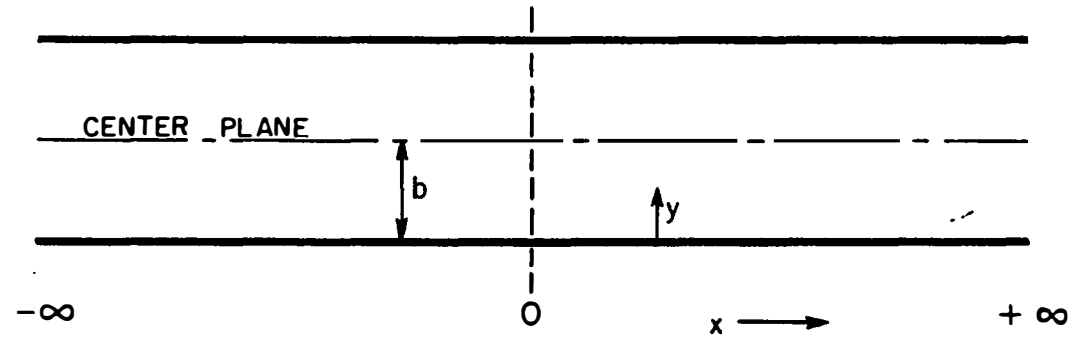

PARALLEL PLATE GEOMETRY

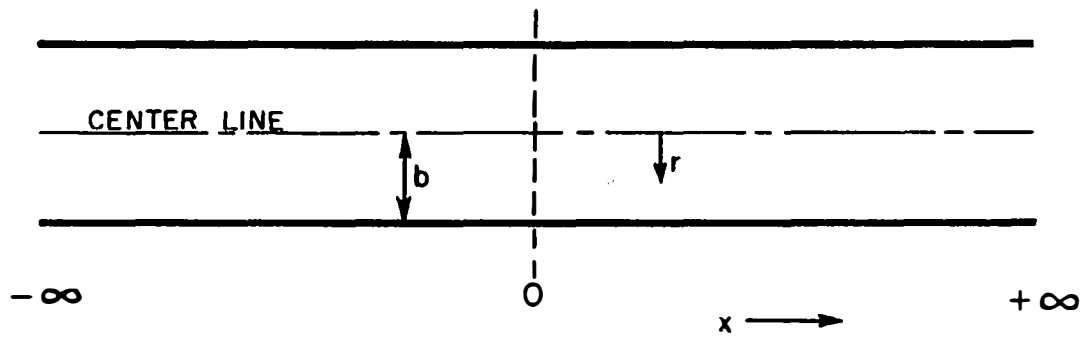

CIRCULAR TUBE GEOMETRY

Fig. 3. Schematic Representation of Parallel Plate And Circular Tube Geometry.

Case I. Fluid temperature is uniform at the entrance. Longitudinal conduction is neglected. (This is the same situation described in Chapter II as the Graetz solution for uniform velocity.)

Referring to Figure 3 for definitions of symbols, the differential equations for Case I may be written as follows:

Parallel Plates

$$U\frac{\partial t}{\partial x} = a\frac{\partial^2 t}{\partial y^2} \qquad \text{III-1}$$

Circular Tubes

$$U\frac{\partial t}{\partial x} = a\left[\frac{\partial^2 t}{\partial r^2} + \frac{1}{r}\frac{\partial t}{\partial r}\right] \qquad \text{III-2}$$

Boundary conditions are:

$t(0,y) = t_o$

$t(x,0) = t_w$

$\frac{\partial t}{\partial y}(x,b) = 0$

$\lim_{x\to\infty} t(x,y) = t_w$

$t(0,r) = t_o$

$t(x,b) = t_w$

$\frac{\partial t}{\partial r}(x,0) = 0$

$\lim_{x\to\infty} t(x,r) = t_w$

Temperature solutions are:

$$\frac{t-t_w}{t_o-t_w} = 4\sum_{n=1}^{\infty}\frac{1}{\beta_n^2}\,e^{-\frac{4\beta_n^2}{Pe_D}x} \qquad \text{III-3}$$

where $\beta_n = (2n-1)\pi$

$$\frac{t-t_w}{t_o-t_w} = 2\sum_{n=1}^{\infty}\frac{J_o\left(\alpha_n\frac{r}{b}\right)}{\alpha_n J_1(\alpha_n)}\,e^{-\frac{4\alpha_n^2}{Pe_D}x} \qquad \text{III-4}$$

where α_n's are roots of $J_o(\alpha_n) = 0$

Local Nusselt moduli are computed according to Equation II-1, as follows:

$$Nu_x = \frac{\sum_{n=1}^{\infty} e^{-\frac{4\beta_n^2}{Pe_D}x}}{\sum_{n=1}^{\infty}\frac{1}{\beta_n^2}\,e^{-\frac{4\beta_n^2}{Pe_D}x}} \qquad \text{III-5}$$

$$Nu_x = \frac{\sum_{n=1}^{\infty} e^{-\frac{4\alpha_n^2}{Pe_D}x}}{\sum_{n=1}^{\infty}\frac{1}{\alpha_n^2}\,e^{-\frac{4\alpha_n^2}{Pe_D}x}} \qquad \text{III-6}$$

Case II. Fluid temperature is uniform at the entrance. Longitudinal conduction is included for positive x.

Parallel Plates

$$U\frac{\partial t}{\partial x} = a\left[\frac{\partial^2 t}{\partial x^2} + \frac{\partial^2 t}{\partial y^2}\right] \qquad \text{III-7}$$

$$t(0,y) = t_o$$

$$t(x,0) = t_w$$

$$\frac{\partial t}{\partial y}(x,b) = 0$$

$$\lim_{x\to\infty} t(x,y) = t_w$$

Circular Tubes

$$U\frac{\partial t}{\partial x} = a\left[\frac{\partial^2 t}{\partial r^2} + \frac{1}{r}\frac{\partial t}{\partial r} + \frac{\partial^2 t}{\partial x^2}\right] \qquad \text{III-8}$$

$$t(0,r) = t_o$$

$$t(x,b) = t_w$$

$$\frac{\partial t}{\partial r}(x,0) = 0$$

$$\lim_{x\to\infty} t(x,r) = t_w$$

$$\frac{t-t_w}{t_o-t_w} = 4\sum_{n=1}^{\infty} \frac{1}{\beta_n} \sin\frac{\beta_n y}{2b}\; e^{\left(\frac{U}{a} - \sqrt{\frac{U^2}{a^2} + \frac{\beta_n^2}{b^2}}\right)\frac{x}{2}} \qquad \text{III-9}$$

$$\frac{t-t_w}{t_o-t_w} = 2\sum_{n=1}^{\infty} \frac{J_o\left(\alpha_n \frac{r}{b}\right)}{\alpha_n J_1(\alpha_n)}\; e^{\left(\frac{U}{a} - \sqrt{\frac{U^2}{a^2} + \frac{4\alpha_n^2}{b^2}}\right)\frac{x}{2}} \qquad \text{III-10}$$

$$Nu_x = \frac{\sum_{n=1}^{\infty} e^{-2\frac{x}{D}\sqrt{\frac{Pe^2}{16}+\beta_n^2}}}{\sum_{n=1}^{\infty} \frac{1}{\beta_n^2} e^{-2\frac{x}{D}\sqrt{\frac{Pe^2}{16}+\beta_n^2}}} \qquad \text{III-11}$$

$$Nu_x = \frac{\sum_{n=1}^{\infty} e^{-2\frac{x}{D}\sqrt{\frac{Pe^2}{16}+\alpha_n^2}}}{\sum_{n=1}^{\infty} \frac{1}{\alpha_n^2} e^{-2\frac{x}{D}\sqrt{\frac{Pe^2}{16}+\alpha_n^2}}} \qquad \text{III-12}$$

Case III. Fluid temperature is initially uniform at $x = -\infty$. The channel wall is maintained at a uniform temperature from $x = -\infty$ to $x = 0$, and at a different uniform temperature from $x = 0$ to $x = +\infty$. The thermal entrance region begins (as in Cases I and II) at $x = 0$.

Parallel Plates

$$U\frac{\partial t}{\partial x} = a\left[\frac{\partial^2 t}{\partial x^2} + \frac{\partial^2 t}{\partial y^2}\right] \qquad \text{III-13}$$

$$\left.\begin{aligned} t(x,0) &= t_1 \\ \lim_{x\to-\infty} t(x,y) &= t_1 \end{aligned}\right\} \quad -\infty < x < 0$$

$$\left.\begin{aligned} t(x,0) &= t_2 \\ \lim_{x\to+\infty} t(x,y) &= t_2 \end{aligned}\right\} \quad 0 < x < +\infty$$

$$\frac{\partial t}{\partial y}(x,b) = 0 \qquad -\infty < x < +\infty$$

Circular Tubes

$$U\frac{\partial t}{\partial x} = a\left[\frac{\partial^2 t}{\partial r^2} + \frac{1}{r}\frac{\partial t}{\partial r} + \frac{\partial^2 t}{\partial x^2}\right] \qquad \text{III-14}$$

$$\left.\begin{aligned} t(x,b) &= t_1 \\ \lim_{x\to-\infty} t(x,r) &= t_1 \end{aligned}\right\} \quad -\infty < x < 0$$

$$\left.\begin{aligned} t(x,b) &= t_2 \\ \lim_{x\to+\infty} t(x,r) &= t_2 \end{aligned}\right\} \quad 0 < x < +\infty$$

$$\frac{\partial t}{\partial r}(x,0) = 0 \qquad -\infty < x < +\infty$$

Parallel Plates **Circular Tubes**

$$\frac{t-t_1}{t_2-t_1} = 1 - 4\sum_{n=1}^{\infty} \frac{1}{\beta_n}\left[\frac{1}{\sqrt{1+\frac{16\beta_n^2}{Pe^2}}}+1\right]\sin\frac{\beta_n Y}{2b}\; e^{\left(\frac{U}{a}-\sqrt{\frac{U^2}{a^2}+\frac{\beta_n^2}{b^2}}\right)\frac{X}{2}} \qquad \text{III-15}$$

$$\frac{t-t_1}{t_2-t_1} = 1 - 2\sum_{n=1}^{\infty} \frac{J_0\left(\alpha_n \frac{r}{b}\right)}{\alpha_n J_1(\alpha_n)}\left[\frac{1}{\sqrt{1+\frac{16\alpha_n^2}{Pe^2}}}+1\right] e^{\left(\frac{U}{a}-\sqrt{\frac{U^2}{a^2}+\frac{\alpha_n^2}{b^2}}\right)\frac{X}{2}} \qquad \text{III-16}$$

$$Nu_x = \frac{\sum_{n=1}^{\infty}\left[\frac{1}{\sqrt{1+\frac{16\beta_n^2}{Pe^2}}}+1\right] e^{-2\frac{X}{D}\sqrt{\frac{Pe^2}{16}+\beta_n^2}}}{\sum_{n=1}^{\infty}\frac{1}{\beta_n^2}\left[\frac{1}{\sqrt{1+\frac{16\beta_n^2}{Pe^2}}}+1\right] e^{-2\frac{X}{D}\sqrt{\frac{Pe^2}{16}+\beta_n^2}}} \qquad \text{III-17}$$

$$Nu_x = \frac{\sum_{n=1}^{\infty}\left[\frac{1}{\sqrt{1+\frac{16\alpha_n^2}{Pe^2}}}+1\right] e^{-2\frac{X}{D}\sqrt{\frac{Pe^2}{16}+\alpha_n^2}}}{\sum_{n=1}^{\infty}\frac{1}{\alpha_n^2}\left[\frac{1}{\sqrt{1+\frac{16\alpha_n^2}{Pe^2}}}+1\right] e^{-2\frac{X}{D}\sqrt{\frac{Pe^2}{16}+\alpha_n^2}}} \qquad \text{III-18}$$

Discussion of Results

Values of local Nusselt modulus computed for the circular tube geometry are shown in Table II. It may be observed from the table that if the Peclet modulus is 400 or greater, the differences between the three cases are negligible. The computed values for Pe = 40 are plotted on Figure 4. Note that differences between the three cases are negligible for values of Pe $\frac{D}{x}$ less than 100. This implies that even at such low Peclet modulus as 40, the effect of longitudinal conduction is negligible for all positions in the entrance region beyond x = 0.4D. In other words, the effect shows itself only in the first increment of length and, even so, it is minor in importance. In considering the range of Peclet modulus involved, it is convenient to recall that it is sometimes defined as the product of the Reynolds modulus and the Prandtl modulus. If one considers a Prandtl modulus of 0.005 (which is about the minimum value for the common liquid metals), the Reynolds modulus corresponding to Pe = 40 is 8000. This may be considered as nearly the minimum Reynolds modulus required to characterize a stream in established turbulent flow. It is believed, then, that Pe = 40 is a lower limit for practical cases of liquid metals in turbulent flow, and the conclusion is that longitudinal conduction is not important in its effect on heat transfer in thermal entrance regions.

It is interesting to note that the solutions for Case I also describe transient conduction in solids initially at uniform temperature and with uniform wall temperature after zero time. These cases are presented by Carslaw and Jaeger (5).

TABLE II

LOCAL VALUES OF NUSSELT MODULUS
FOR CIRCULAR TUBE GEOMETRY

$Pe \frac{D}{x}$	Case I	Case II		Case III	
		Pe = 40	Pe = 400	Pe = 40	Pe = 400
10	5.78	5.78	5.78	5.78	5.78
40	6.17	6.27	6.17	6.25	6.17
100	7.74	8.08	7.73	7.94	7.73
400	13.08	15.24	13.09	14.08	13.08
1000	19.50	26.72	19.74	22.72	19.57

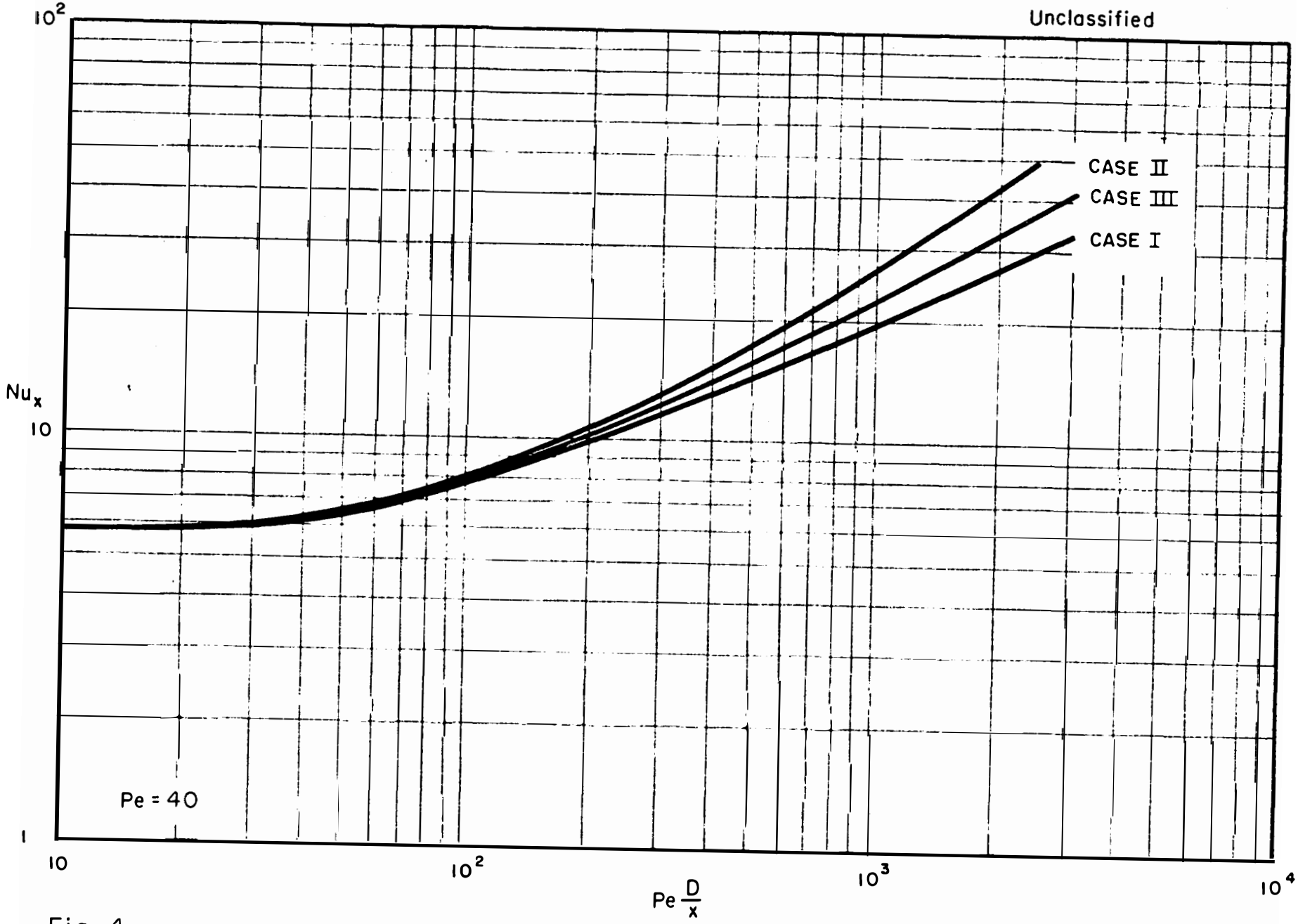

Fig. 4. Comparison of Solutions Including the Effect of Longitudinal Conduction

CHAPTER IV

DESCRIPTION OF THE EXPERIMENTAL SYSTEMS

In the course of the present work, two different experimental systems were employed in order to study the thermal entrance region heat transfer to liquid metals. However, in both systems, the same test section was employed.

Heat Transfer Test Section

The test section is shown in cross-section on Figure 5. It may be considered as a short, thick-walled copper cylinder (with a 3 inch outside diameter, 1/16 to 1/8 inch length, 1/16 to 1/8 inch inside diameter) mounted between stainless steel flanges with 3/8 inch by 1/4 inch thick Hycar hard rubber gaskets. The stainless flanges were tapped with standard 1/4 inch pipe threads in which were inserted 1/4 inch pipe to 3/8 inch tube connectors containing thermowells. Thus, in order to remove the test section assembly from the experimental systems, it was only necessary to loosen two tubing flare nuts.

Mercury Heat Transfer System

The system in which this test section was installed for determining the heat transfer coefficients to mercury is shown schematically on Figure 6. The sump consisted of a rectangular stainless steel vessel, approximately 10 inches deep, 12 inches long and 8 inches wide with a 1/8 inch thick wall. From this vessel, mercury was pumped by means of a small turbine pump through a cooler (consisting of a coil submerged in a tank of water) and then through the test section. After

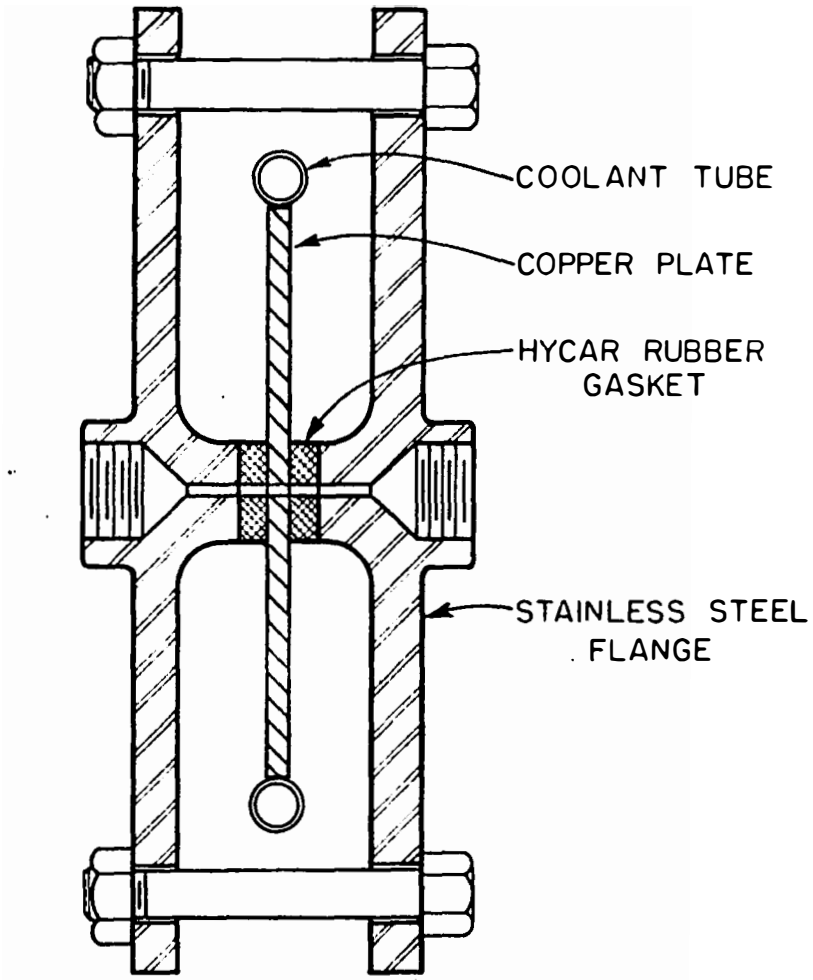

Fig. 5. Sectional View of Test Section Assembly

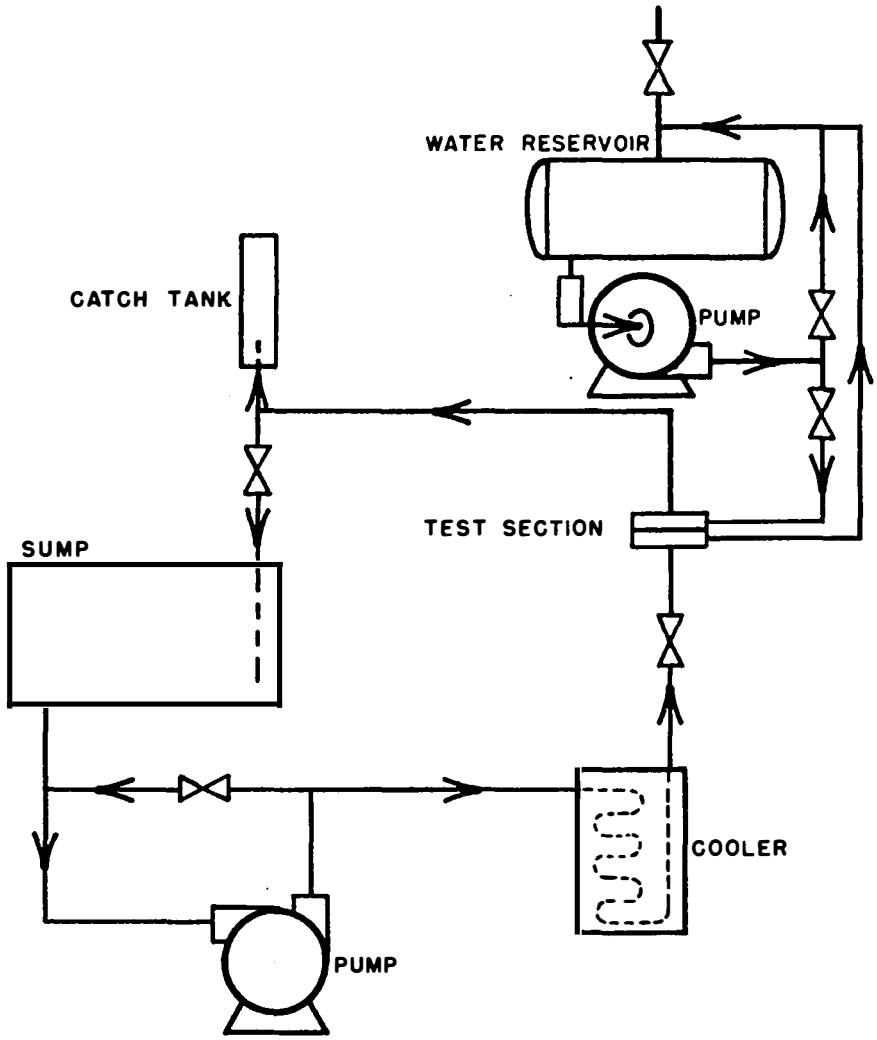

Fig. 6. Schematic Diagram of Mercury Heat Transfer System

the mercury passed through the test section, it could be diverted to a catch tank in which flow rate measurements are made, or it could be returned to the sump. In the catch tank were located two probes which completed electrical circuits, turning on and turning off a timer when the mercury reached fixed levels in the tank. After the system was degreased with trichlorethylene and acetone washes, approximately 100 pounds of triple distilled mercury was loaded into the sump. A nitrogen atmosphere was introduced above the mercury in the sump so as to minimize oxidation. Main flow channels consisted of 3/8 inch outside diameter stainless steel tubing. The flow rate was controlled by a 3/4 inch bypass valve and small adjustments were made with a 1/4 inch globe valve in the main circuit.

Auxiliary Water System

In order to insure that the periphery of the copper plate in the test section was maintained at a uniform temperature, an auxiliary water system was constructed. In this system, water temperature was controlled by a bimetallic thermoregulator located in a mixing chamber in the supply line to the test section. This regulator, through a relay circuit, operated an immersion type resistance heater located in the water reservoir. A pressure limit switch was included in the heater relay circuit so as to break the circuit if the pressure exceeded 5 psi. As an added precaution, a 25 psi pop-off valve was provided in case excessive pressure built up in the water reservoir for any reason. A

laboratory size centrifugal pump was used to circulate the hot water through the tube around the copper plate in the test section.

Temperature Measurement System

Other auxiliary equipment included the temperature measuring apparatus. Precise measurement of the temperature was required in the test section for determining the heat transfer rate and the copper surface temperature. No. 30 constantan wires were soldered through 1/64 inch diameter holes drilled in the copper plate at locations indicated on Figure 7. A copper lead was soldered to the surface of the plate, and the plate itself served as a common copper lead to all the constantan junctions. The leads were passed to an enclosed terminal strip for selection by a Leeds and Northrup thermocouple switch, and the circuit continued through an ice bath cold junction to a Rubicon type B potentiometer. A General Electric type 32C240G14 galvanometer was used in connection with the potentiometer. Mercury and water temperatures were measured upstream and downstream from the test section by means of copper-constantan couples in thermowells. The potentiometer system described above was also used for these measurements.

Sodium Heat Transfer System

A diagram of the sodium heat transfer system is shown on Figure 8. The sump and reservoir were both made from 10 inch, schedule 40, black iron pipe, and they were each provided with a hot plate at the bottom and strip heaters around the outside surface. The main flow channels

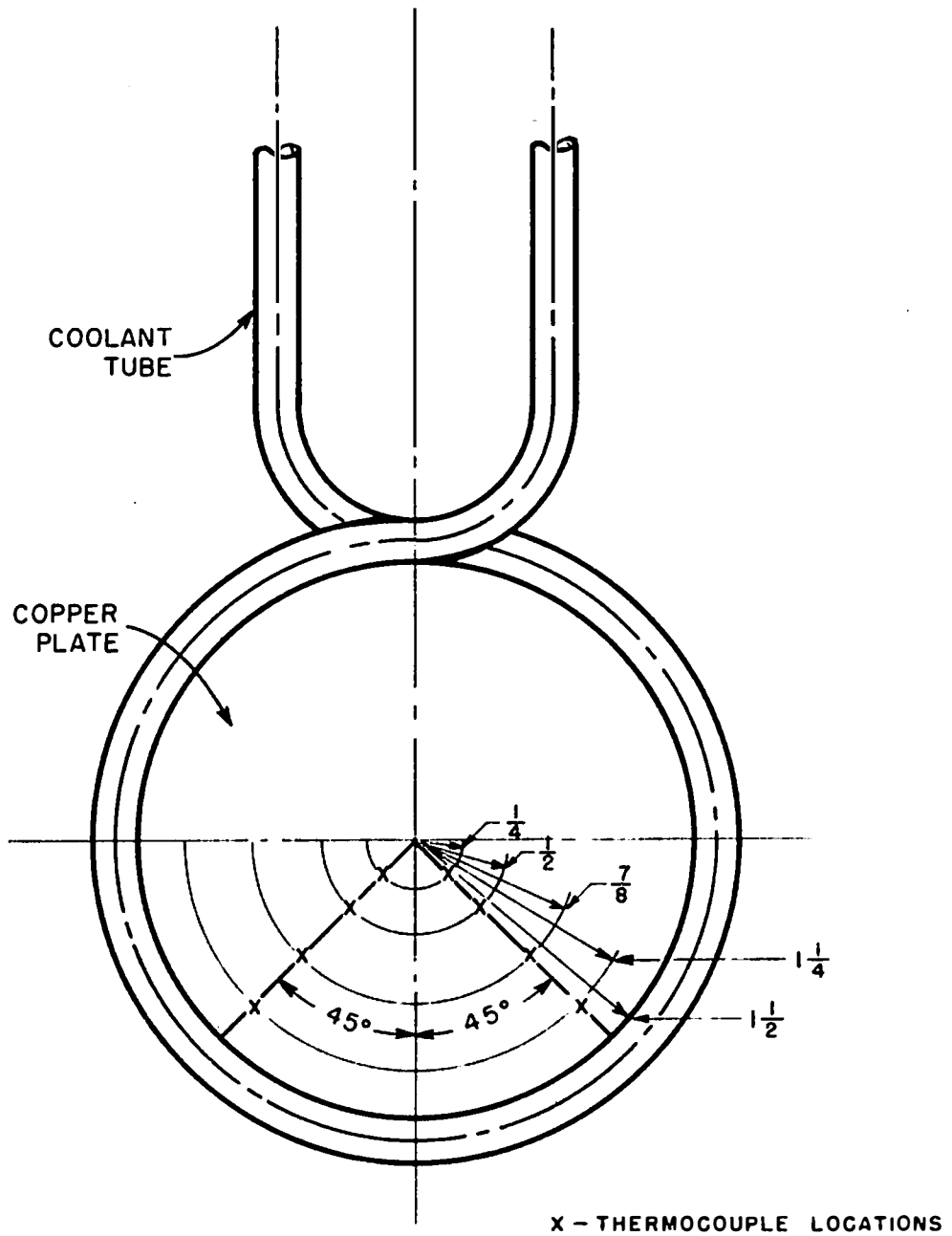

Fig. 7. Thermocouple Locations in Test Section Plate

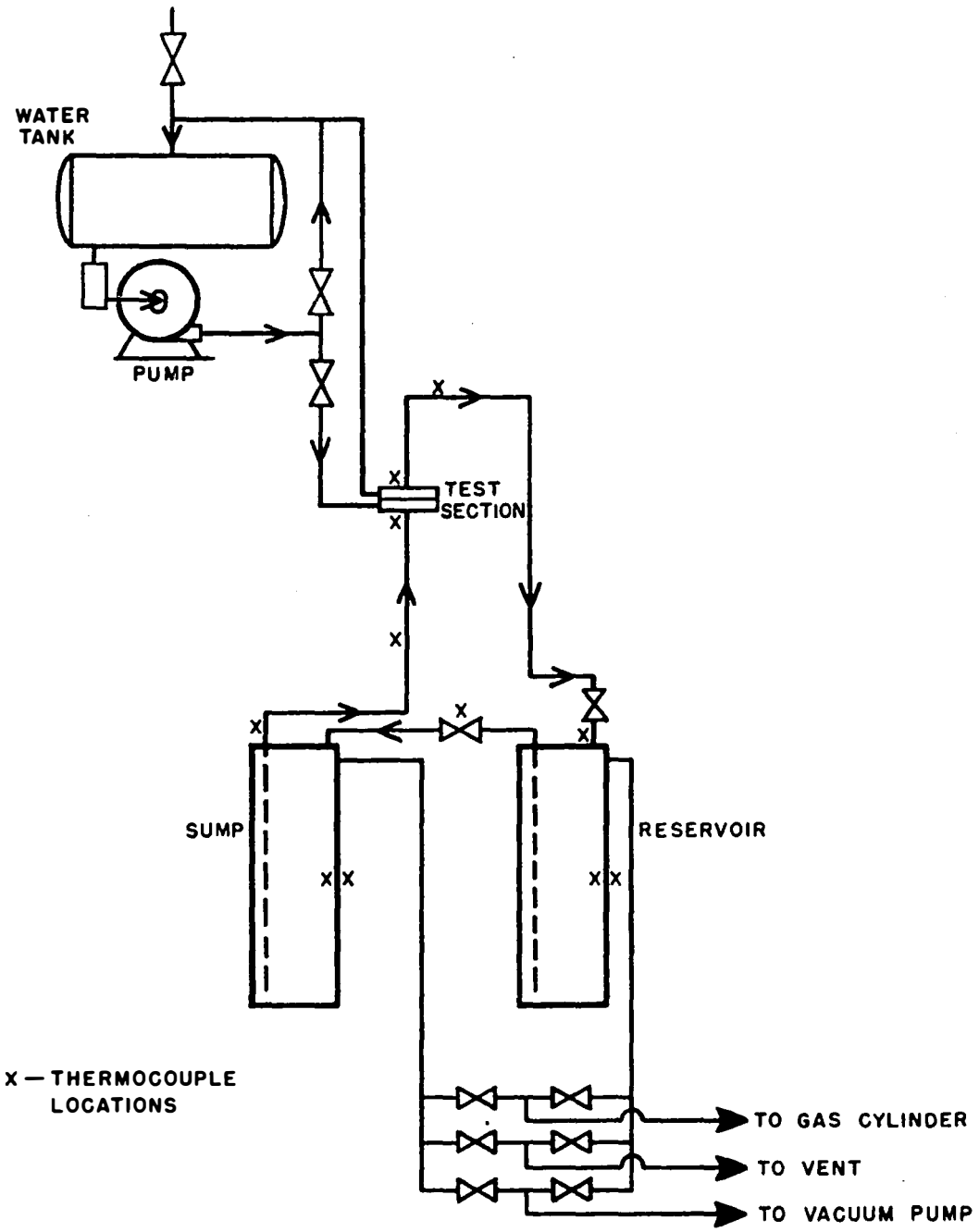

Fig. 8. Schematic Diagram of Sodium Heat Transfer System

were of 3/8 inch outside diameter stainless steel tubing. The tubing and stainless steel valves were wound with monel-sheathed, asbestos covered, No. 14 Nichrome resistance wire. Argon was used as an inert atmosphere over sodium within the system. It was also used to displace the sodium from the sump through the test section circuit to the reservoir, and from the reservoir to the sump through the return circuit. A standard gas cylinder served as the argon source and a regulator was used to control the pressure in the system. A vacuum pump was used to evacuate the system at the initial loading of the sodium and following any changes in the system which would have permitted entry of air. All heater circuits were controlled by variable transformers, or, in some cases by variable resistors. In order to determine thermal conditions throughout the system, temperatures were measured at strategic locations by means of iron-constantan thermocouples operating through a 12 point self-balancing temperature indicator. These thermocouple locations are indicated on Figure 8.

The auxiliary water system and temperature measuring circuits, which have already been described, were also used with the sodium system. As in the mercury system, sodium temperatures were measured upstream and downstream from the test section by means of copper-constantan couples in thermowells.

Operation of the mercury system was straightforward, but the sodium system required special attention. Prior to loading, the sodium system was flushed with trichlorethylene for degreasing and

removal of foreign particles. It was then thoroughly dried and filled with argon in preparation for loading the sodium. Seven 12 pound bricks of sodium were then scraped in an argon atmosphere in order to remove the oxide layer coating the bricks. These bricks were then loaded into the reservoir which was continuously flushed with an argon stream during this operation. After the bricks were placed in the reservoir, the top flange was secured and the system was evacuated and purged with argon in order to remove any air which may have been retained. Heater circuits were then closed in order to melt the sodium and preheat the flow circuits. The test section was preheated partly by conduction from the adjoining tubing heaters, partly by guard heaters at the outside faces of the flanges, and partly through circulation of pressurized hot water through the tube at the periphery of the center plate. When temperature readings indicated that the sump, reservoir, and flow channels were sufficiently hot and that the sodium was completely melted (m.p. 208°F.), the sodium in the reservoir was transferred to the sump by displacement with argon. Preparation for an actual run consisted of closing the valve in the return circuit, opening the valve in the test section circuit, adjusting the argon regulator to the desired operating pressure, and opening the vent valve from the reservoir. A run began upon opening the valve from the argon supply to the sump.

Steady conditions were obtained quickly as shown by the change of temperature readings in the test section during the first minute of

operation.[1] The volumetric flow rate of the sodium was determined by the use of four probes located at different elevations in the reservoir. The sodium completed an electrical circuit when it contacted each probe, and, by means of a relay circuit, a timer (reading to 0.1 seconds) was started and stopped automatically. The two bottom probes and the two top probes were paired so as to get two independent flow rate determinations for each run.

Operative Problems

Operative problems which developed were chiefly in two regions: (1) assembly of the test section; and, (2) presence of oxides in the sodium.

The problem of assembly of the test section may be clarified by considering the cross-sectional view of the assembly as shown on Figure 5. The extent of compression of the gaskets necessary to hold 300 psi internal pressure was determined roughly by a hydrostatic test. Each gasket was then placed between the flanges and the center hole was drilled while the gasket was compressed to a specified thickness. The center hole in the plate was carefully drilled prior to assembly, and the assembly operation was performed by stacking flange, gasket, plate, gasket, and flange in a sandwich aligned by a drill through the center.

---

1. This observation confirmed a graphical prediction based on the methods of Perry and Berggren (29). See Chapter V.

After the flange bolts were tightened to again compress the gaskets to the proper thickness, the drill was removed and the center hole was washed with a detergent. It was then ready for installation in the test section circuit.

Preliminary work indicated that sufficient oxygen was in the system to saturate the sodium with sodium oxide. This oxygen presumably came from residual oxygen adsorbed to surfaces within the system, residual oxide not removed from bricks before loading, and traces of oxygen in the argon gas. In order to prevent precipitation of oxide on the heat exchange surface, part of the runs were made with the sump at a lower temperature than the surface temperature of the test section, and some data were taken for heating sodium as well as for cooling.

The experimental results obtained in these two heat transfer systems are discussed in the next chapter.

CHAPTER V

EXPERIMENTAL RESULTS

In Chapter IV, the experimental systems employed in these heat transfer studies were described. Data taken during each experimental run included the following:

1. Liquid metal temperature upstream and downstream from the test section.
2. Hot water or steam temperature upstream and downstream from the test section.
3. Temperatures at two points for each of four different radial positions on the copper plate in the test section.
4. Timer readings to be used to compute the volumetric flow rate of the liquid metal.

During operation of the experimental apparatus, the liquid metal being studied was circulated through the center hole in the copper plate within the test section.[1] Pressurized hot water or steam was circulated through the tube at the periphery of the copper plate so as to maintain the periphery at essentially constant temperature. The flat sides of the copper plate were insulated so that, as a result of the high thermal conductivity of the copper, radial heat flow was achieved in the plate. From temperature measurements made at different radial positions,

---

1. See Figure 5

the rate of heat transfer and the copper temperature at the copper-sodium interface were determined according to the relation[2]

$$q = \frac{2\pi kL(t-t_w)}{\ln \frac{r}{b}} \qquad \text{V-1}$$

A simple graphical procedure may be used in the analysis by re-arranging Equation V-1 to the form

$$t = t_w + \frac{q}{2\pi kL} \ln \frac{r}{b} \qquad \text{V-2}$$

By plotting temperature at a given radius versus the logarithm of the ratio of that radius to the radius of the flow channel, one obtains a linear relationship with a slope of $\frac{q}{2\pi kL}$ and intercept of t_w. The arithmetic average of the upstream and downstream liquid metal temperature measurements was taken as the mean fluid temperature within the test section. These data were then used to compute the average heat transfer coefficient throughout the length of the channel (plate thickness), according the the relation

$$h_L = \frac{q}{A(t_m-t_w)} \qquad \text{V-3}$$

In order to estimate the time required for steady conditions to be attained in the test section, a graphical analysis was made according to the method of Perry and Berggren (29). The results indicated that, after the first five seconds, the largest difference between the

---

2. Thermal conductivity of copper is constant within 1% over the temperature range in the plate.

graphically determined transient temperature and the steady state temperature is half of one percent of the radial temperature difference initially imposed on the plate at zero time.

The data, obtained in three different test sections for heat transfer to mercury in the thermal entrance region, are summarized in Table III and plotted on Figure 9[3]. For comparison, three solutions described in Chapter II are also plotted on Figure 9. Since the solutions plotted are dependent on molecular conduction alone, the upward trend of the data (compared with these solutions) for high values of Pe $\frac{D}{L}$ is attributed to the contribution of eddy conduction which increases as the Reynolds modulus increases.

Since comparison is made between the experimental data and analytical conduction solutions, it is desirable to determine how closely the experimental system fits the description of the ideal system postulated in the mathematical analysis. One tacit assumption in the ideal system is that the flow channel upstream from the heated section is adiabatic. In order to determine (1) whether or not this is so in the experimental system; (2) whether or not the radial heat flow in the test section plate is a true indication of the heat input to the liquid; and (3) whether or not the area of the center hole in

---

3. Two plots appearing on Figure 9 differ by the choice of thermal conductivity data. Data of Hall (15) are believed to be more reliable than the data of Gehlhoff and Neumeier (12). Other physical properties are shown in Appendix D.

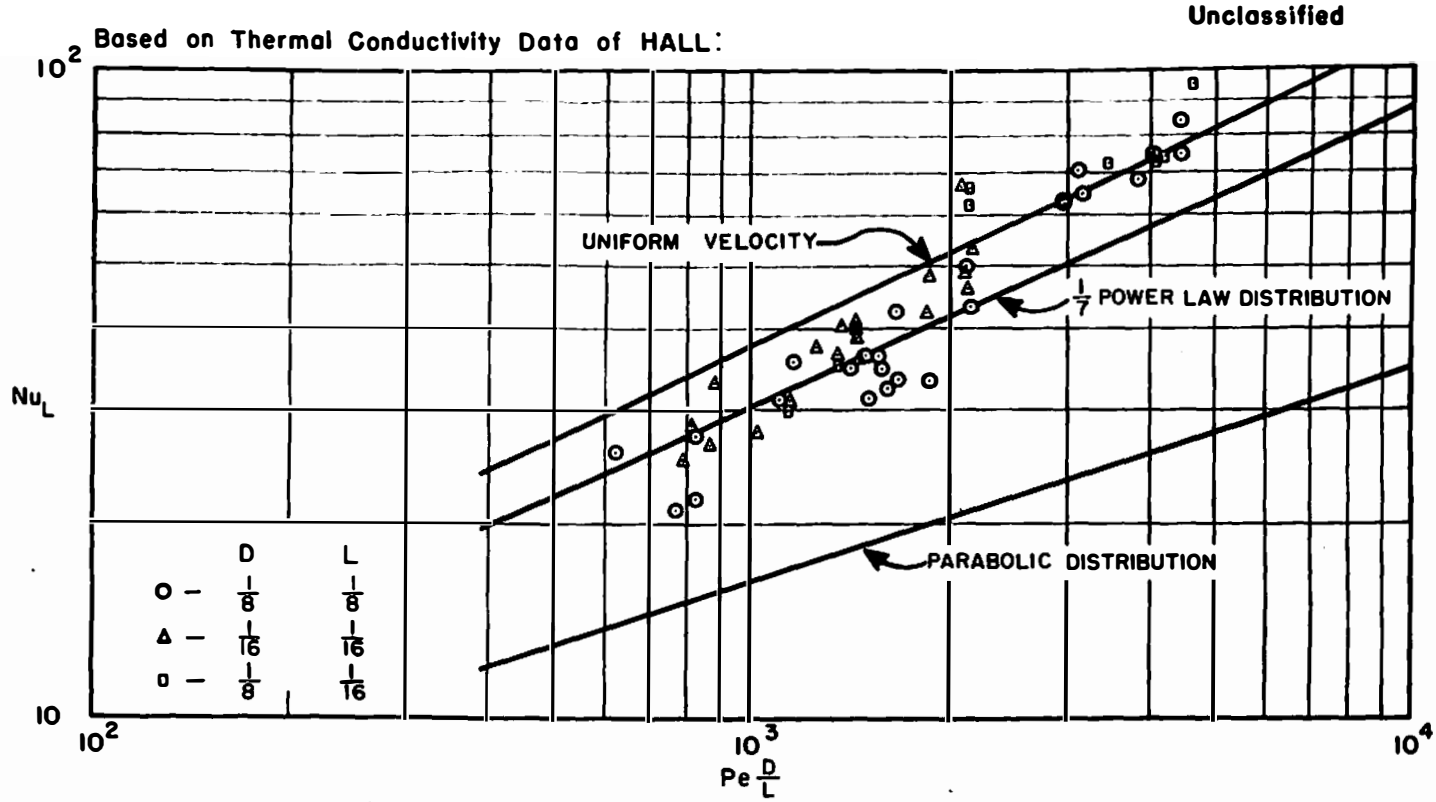

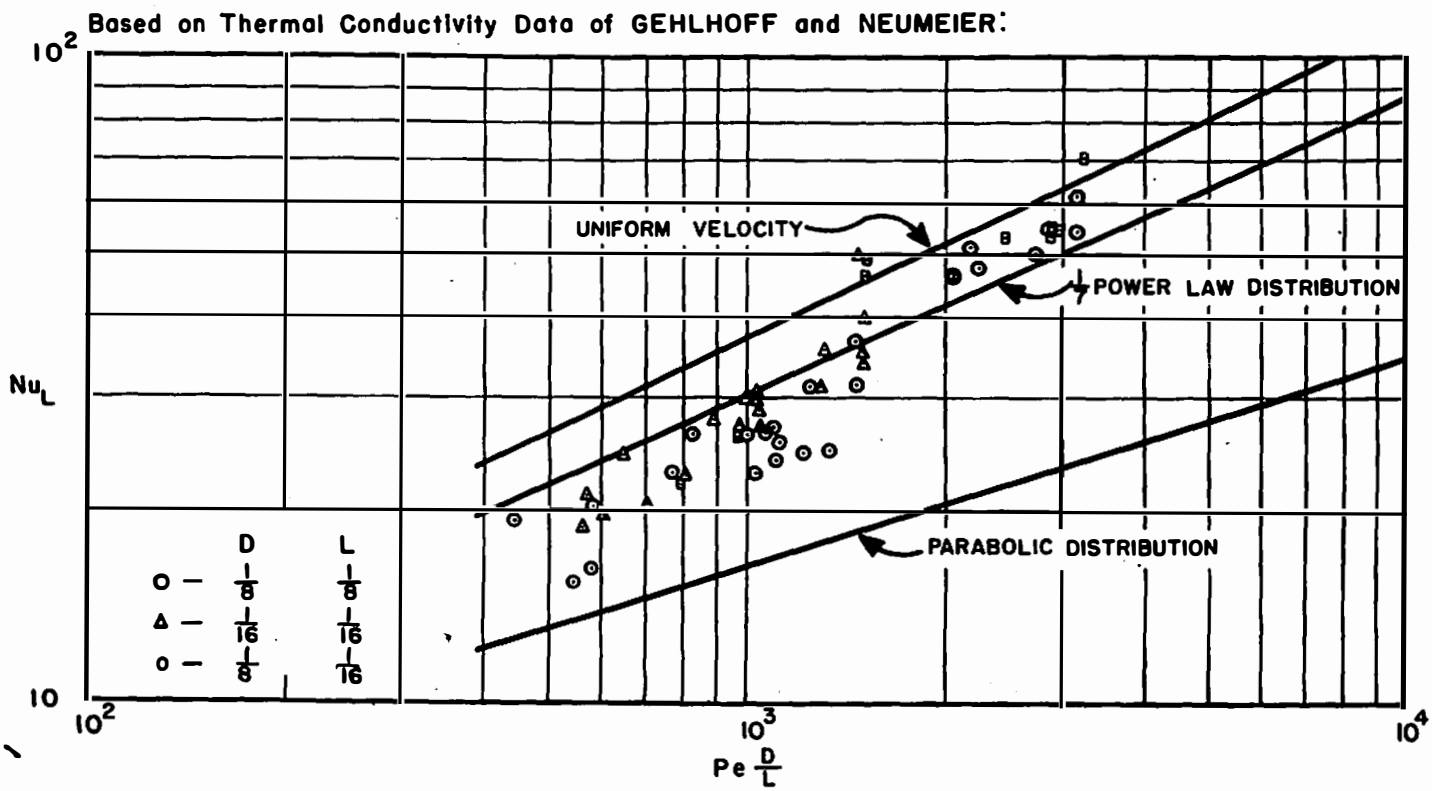

Fig. 9. Heat Transfer to Mercury in a Thermal Entrance Region.

TABLE III

SUMMARY OF MERCURY HEAT TRANSFER DATA

Run	D, in.	L, in.	t_m, °F	Re	h, Btu/hr.ft.^{2} °F	Nu_L*	Pe $\frac{D}{L}$*	Nu_L**	Pe $\frac{D}{L}$**
1	1/8	1/8	75.4	58900	17150	26.3	1000	35.0	1415
2	1/8	1/8	77.3	78500	16500	25.0	1330	33.7	1870
3	1/8	1/8	78.2	71000	16500	24.9	1210	33.5	1685
4	1/8	1/8	77.9	63400	17900	26.6	1078	36.5	1500
5	1/8	1/8	70.8	45200	15150	23.2	769	31.2	1105
6	1/8	1/8	74.2	64600	17950	27.1	1100	36.7	1560
7	1/8	1/8	75.6	65700	17100	25.8	1120	34.9	1580
8	1/8	1/8	70.4	32100	10300	15.75	546	21.1	776
9	1/8	1/8	71.3	34200	10700	16.35	581	22.0	835
10	1/8	1/8	71.6	26200	12650	19.4	445	26.0	636
11	1/8	1/8	71.8	34300	13500	20.4	583	27.7	833
12	1/8	1/8	74.6	48600	17500	26.4	827	35.7	1165
13	1/8	1/8	92.2	197000	37700	54.9	3150	75.1	4430
14	1/8	1/8	91.3	197000	42600	62.0	3150	84.7	4450
15	1/8	1/8	89.7	177500	37800	55.1	2840	75.7	4050
16	1/8	1/8	90.5	140000	32900	48.0	2240	65.8	3180
17	1/8	1/8	90.8	137000	35400	51.5	2190	70.8	3110
18	1/8	1/8	91.9	170000	34500	50.4	2720	68.8	3840
19	1/8	1/8	87.3	129000	31900	46.8	2060	64.0	2970
20	1/8	1/8	87.7	129000	31600	46.4	2060	63.4	2970
21	1/8	1/8	84.1	92500	21400	31.5	1480	43.3	2150
22	1/8	1/8	84.3	91600	24900	36.8	1465	50.2	2125
23	1/8	1/8	83.3	71100	21200	31.6	1240	42.9	1660
24	1/8	1/8	83.4	69000	16200	24.1	1105	32.7	1610
25	1/8	1/8	82.3	64800	15600	23.2	1035	31.6	1520
26	1/16	1/16	88.4	35600	28600	21.2	569	28.7	815
27	1/16	1/16	80.4	53800	37300	27.7	888	37.8	1265
28	1/16	1/16	75.0	36700	32300	24.4	624	33.0	881
29	1/16	1/16	72.0	47500	29200	22.8	807	31.0	1155

TABLE III (CONTINUED)

SUMMARY OF MERCURY HEAT TRANSFER DATA

Run	D, in.	L, in.	t_m, °F	Re	h, Btu/hr.ft.^{2} °F	Nu_L*	Pe $\frac{D}{L}$*	Nu_L**	Pe $\frac{D}{L}$**
30	1/16	1/16	74.0	88300	45300	34.2	1500	46.3	2125
31	1/16	1/16	74.2	89400	52400	39.6	1520	53.5	2155
32	1/16	1/16	66.0	40900	26900	20.6	715	27.9	1020
33	1/16	1/16	72.7	76500	41500	31.3	1300	42.5	1850
34	1/16	1/16	72.8	76800	47100	35.5	1310	48.3	1860
35	1/16	1/16	71.4	59700	37900	28.8	1045	38.9	1450
36	1/16	1/16	71.1	60000	35600	27.1	1050	36.7	1465
37	1/16	1/16	70.0	59000	40000	30.5	1033	41.2	1445
38	1/16	1/16	69.9	59100	39200	29.8	1033	40.4	1450
39	1/16	1/16	66.4	32100	24600	18.9	562	25.4	795
40	1/16	1/16	67.0	34900	25800	19.75	611	26.7	866
41	1/16	1/16	70.8	56600	39500	30.0	990	40.6	1380
42	1/16	1/16	70.5	55700	35800	27.2	975	36.8	1360
43	1/16	1/16	75.3	87100	66300	50.0	1480	67.6	2090
44	1/16	1/16	75.1	88300	48000	36.2	1500	49.0	2120
45	1/8	1/16	79.0	24100	14750	22.0	795	30.0	1140
46	1/8	1/16	74.2	28400	17400	26.2	965	35.5	1370
47	1/8	1/16	75.1	44500	32800	49.5	1515	67.0	2135
48	1/8	1/16	75.7	44500	30700	46.4	1515	62.8	2135
49	1/8	1/16	79.8	87100	36200	54.0	2880	73.5	4110
50	1/8	1/16	82.4	90400	37000	55.0	2980	74.8	4230
51	1/8	1/16	82.4	87200	37100	55.2	2880	75.0	4080
52	1/8	1/16	85.3	100500	48000	70.5	3220	96.5	4650
53	1/8	1/16	82.8	75000	36100	53.3	2470	72.8	3490

* Based on thermal conductivity data of Gehlhoff and Neumeier (12).

** Based on thermal conductivity data of Hall (15).

the plate is the effective heat transfer area, a brief analysis was made of the conduction of heat across the corner of the hard rubber gaskets which hold the test plate in position. This analysis is shown in Appendix E, and the conclusion drawn from it is that the heat leak across the gasket amounts to less than 1% of the radial heat flow in the test plate. This conclusion makes it appear that the experimental system closely approximates the ideal system with respect to the considerations mentioned above.

Another item of great importance is the variation of wall temperature in the test section. The analytical solutions with which the data are compared are based on the postulate of uniform wall temperature. In order to estimate the variation of wall temperature in the experimental system, an iterative procedure was employed in two examples as shown in Appendix F. Results of this study showed that the average deviation of the temperature from a uniform value is about 3.3% of the difference between the surface temperature and the mean fluid temperature for a run having an average heat transfer coefficient of 8220 Btu/hr. ft.^{2} $^\circ$F. For runs having an average heat transfer coefficient of 77,290 Btu/hr. ft.^{2} $^\circ$F., the temperature distribution is intermediate between the uniform temperature case and the uniform wall heat flux case. The average deviation in wall temperature in this case is about 19%. These two examples bracket the range of experimentally measured heat transfer coefficients to mercury. The influence of the temperature deviation in the high heat transfer coefficient example would be to increase the predicted values. It can be shown for uniform velocity

systems that predictions based on the postulate of uniform wall temperature are only about 70% of those based on the postulate of uniform flux. The contribution of the eddy conduction is believed to be the more important factor, however, in accounting for the increasing deviation of the data from the conduction solutions as the value $Pe \frac{D}{L}$ is increased.

In view of (1) the high thermal conductivity of the copper path from the tube at the periphery of the test plate to the center hole, and (2) the estimation that less than 1% of the radial heat flow is conducted across the gasket corner, considerable confidence is placed in the rate of heat flow as computed from the temperature gradient in the plate. In an effort to obtain a heat balance, the liquid metal stream temperatures were measured upstream and downstream from the test section. The temperature changes in the stream were so small that conduction errors in the thermowells became significant. Hence, no confidence was placed in these measurements for the heat balance, but they were used to obtain the mean liquid temperature. In effect, the copper plate was used as a heat meter, and it is believed that the uncertainty in the heat rate determined in this way is small compared with other uncertainties of the system.

With regard to other uncertainties of the system, an error analysis is made in Appendix G. Since three different test sections were employed in obtaining the experimental data, the analysis for precision includes consideration of physical size and thermocouple

location as well as the quantities measured during each experimental run. Results of the error analysis indicated a precision of about 2% in Nusselt modulus when plotted against the modulus, Pe $\frac{D}{L}$. The accuracy is uncertain primarily to the same extent that the physical properties (particularly thermal conductivity) are uncertain. This point is illustrated by the wide deviation between the two sets of thermal conductivity data for mercury, as shown in Appendix D along with other pertinent physical properties of both mercury and sodium.

The present study was undertaken as a study of heat transfer in a thermal entrance region as distinguished from a combined thermal and hydrodynamic entrance region. However, the system which was evolved and operated did not incorporate a very long calming section upstream from the test section. For the channels of 1/8 in. diameter the calming section was about four diameters long, and for the 1/16 in. diameter channels it was about eight diameters long. Clearly, by usual standards, these lengths are not considered adequate for establishing the velocity distribution. However, it may be noted that in the test sections of L=D= 1/16 in. and L=D = 1/8 in., the $\frac{L}{D}$ ratios are the same but the hydrodynamic calming section is twice as long for the 1/16 in. channel as for the 1/8 in. channel. There is no appreciable difference between the experimental results obtained from these two test sections, indicating that the hydrodynamic entrance effect is negligible for these studies.

A set of sample calculations is presented in Appendix C, showing the treatment of the experimental data for comparison with the analytical solutions.

As shown in Table III, the Nusselt moduli for mercury, based on the thermal conductivity data of Hall, ranged from 21.1 to 96.5. It was expected that Nusselt moduli in the same range should be achieved for sodium. This would imply that, compared to heat transfer coefficients of 10,300 to 66,300 Btu/hr. ft^2 ^oF. for mercury, the attainable heat transfer coefficients to sodium should be about nine times these values--up to about 600,000 Btu/hr. ft^2 ^oF. However, the sodium data were not reproducible and were very low and erratic. The region in which these data fell is compared with the region of mercury data on Figure 10, and the data are summarized in Table IV. Heat transfer coefficients up to 73,600 Btu/hr. $ft.^2$ ^oF. were achieved but these were still extremely low when compared with the region of Nusselt moduli in which the mercury data fell. Clearly the attainment of coefficients of the order of 100,000 to 600,000 Btu/hr. $ft.^2$ ^oF. puts a premium on good interfacial contact, but the role of eddy conductivity and velocity distribution would be expected to be the same for both sodium and mercury. In the next chapter, a few comments will be made regarding interfacial contact between sodium and copper.

Unclassified

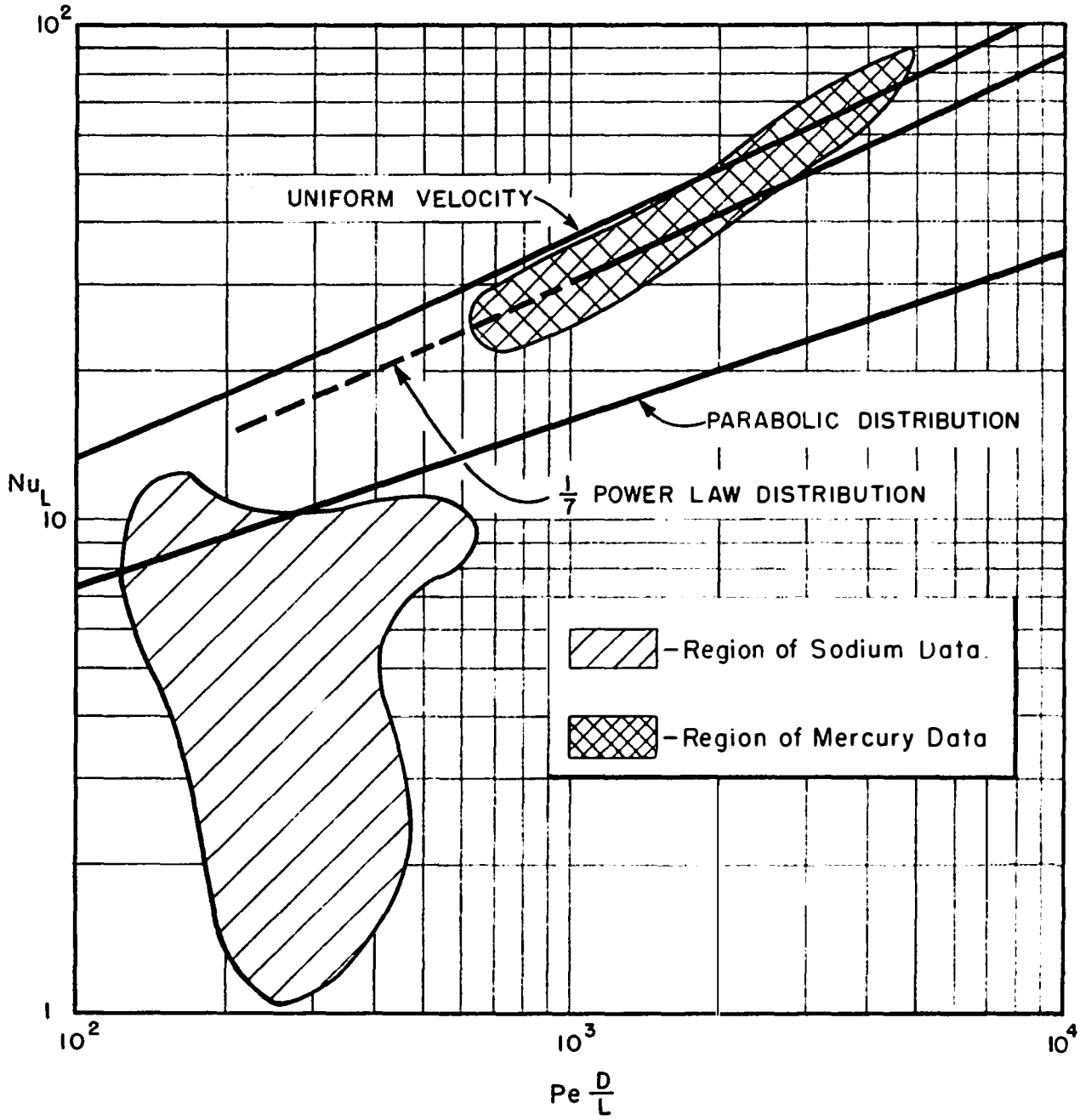

Fig. 10. Region of Sodium Data Relative to the Mercury Data.

TABLE IV

SUMMARY OF SODIUM HEAT TRANSFER DATA

Run	D, in.	L, in.	t_m, °F	Re	h, Btu/hr.ft.^{2} °F	Nu_L	Pe $\frac{D}{L}$
1	1/16	1/8	300	49500	23500	2.54	219
2	1/16	1/8	307	45000	30400	3.30	200
3	1/16	1/8	306	50500	31500	3.42	223
4	5/64	1/8	293	55800	66900	9.05	314
5	5/64	1/8	292	57500	55500	7.50	324
6	5/64	1/8	290	57200	66500	8.98	324
7	3/32	1/8	294	55000	59700	9.67	371
8	3/32	1/8	289	37000	36900	5.98	251
9	3/32	1/8	280	27400	15900	2.58	189
10	3/32	1/8	250	28200	13500	2.14	210
11	3/32	1/8	283	26800	20350	3.30	184
12	3/32	1/8	280	51500	31300	5.08	355
13	3/32	1/8	282	32600	13800	2.24	225
14	3/32	1/8	285	70400	13000	2.11	482
15	3/32	1/8	287	45100	19100	3.10	308
16	3/32	1/8	291	86100	68600	11.1	585
17	3/32	1/8	288	51400	58800	9.52	349
18	3/32	1/8	290	95200	51600	8.36	647
19	3/32	1/8	289	37800	42800	6.93	256
20	3/32	1/8	287	39800	22900	3.71	272
21	3/32	1/8	288	61700	45200	7.32	420
22	3/32	1/8	286	24300	62100	10.1	167
23	3/32	1/8	285	22300	30900	5.01	153
24	3/32	1/8	289	30400	43100	7.0	206
25	1/16	1/16	280	39300	14750	1.59	370

TABLE IV (CONTINUED)

SUMMARY OF SODIUM HEAT TRANSFER DATA

Run	D, in.	L, in.	t_m, °F	Re	h, Btu/hr.ft.^{2} °F	Nu_L	Pe $\frac{D}{L}$
26	1/16	1/16	278	45000	24000	2.60	426
27	1/16	1/16	254	36600	42700	4.53	369
28	1/16	1/16	265	23800	16850	1.80	235
29	1/16	1/16	261	23200	12800	1.37	230
30	1/16	1/16	310	30600	9830	1.06	272
31	1/16	1/16	285	33700	15520	1.67	316
32	1/16	1/16	297	33800	16200	1.75	307
33	1/16	1/16	282	34900	14500	1.55	329
34*	1/16	1/16	254	32100	10600	1.12	324
35*	1/16	1/16	252	28400	22600	2.40	287
36*	1/16	1/16	257	37700	18200	1.93	379
37*	1/16	1/16	258	44500	35500	3.77	446

* Heating runs

CHAPTER VI

AN EXPLANATION OF THE SODIUM DATA

In the last chapter, it was pointed out that the experimental results obtained with sodium were low and inconsistent. Since the bulk of the data fell below the conduction solutions (even the solution for parabolic velocity distribution), it appeared that an additional thermal resistance of variable magnitude was showing itself in the thermal circuit. In the present studies, the thermal circuit was well defined from the peripheral tube in the test section to the hole interface bounded by the copper and filled with sodium. The temperature field and heat flow in the copper plate were measured experimentally. Hence the region of uncertainty began at the copper surface of known temperature and extended into the fluid. If intimate contact was made between the copper and sodium, it is hard to conceive of a situation which would yield data lower than values predicated on the postulates of zero eddy conduction and parabolic velocity distribution, when the lowest Reynolds modulus employed was about 20,000.

For purposes of examining the influence of poor interfacial contact, consider this condition to be represented as a series resistance of thickness x and conductivity k_x. If the heat transfer areas are approximately equal,

$$\frac{1}{h_o} = \frac{x}{K_x} + \frac{1}{h_c} \qquad \text{VI-1}$$

where subscripts o and c refer to observed and computed values, respectively. This equation may be arranged to get the following:

$$\frac{h_c}{h_o} = \frac{x}{k_x} h_c + 1 \qquad \text{VI-2.}$$

or

$$\frac{Nu_c}{Nu_o} = \frac{x}{k_x} \frac{k_f}{D} Nu_c + 1 \qquad \text{VI-3.}$$

where k_f is the thermal conductivity of the heat transfer fluid and D is the channel diameter. Equation VI-3 shows the importance of having a very low value of $\frac{x}{k_x}$ in the present studies, since k_f of sodium is very high (about 50 Btu/hr. ft.^{2} ^oF/ft. at its m.p.) and the channel diameter was as small as 1/16 inch. In order to observe values equal to the computed values, x must be zero or very small. Attempts were made to improve the sodium data by carefully cleaning and electropolishing the copper heat transfer surface, as well as by revising procedures of assembly in the test section. In order to eliminate the possibility that sodium oxides were precipitating on the test surface, heating runs were made but these resulted in no significant change in the data. It was finally suspected that the additional unknown thermal resistance existing at the interface consisted of oxides coating the copper surface. This appeared to contradict previous accounts of the use of sodium for deoxidizing copper, but it was later concluded that this use is confined to copper melts rather than surfaces of solid copper.

Copper is known to have a great affinity for oxygen and hot copper shavings are often used to deoxidize gas streams. In every case, the copper surface was cleaned and dried in air so that all surfaces were air-oxidized at room temperature. Moyer and Riemen (28) con-

ducted measurements of heat transfer across a sodium-stainless steel interface in three pieces of apparatus and concluded that wetting played little part, if any, in their experiments. However the minimum interfacial resistance detectable in their work (corresponding to the limit of precision of their measurements) was equivalent to 0.010 in. of stainless steel. In terms of a heat transfer coefficient, this is roughly equal to 12,000 Btu/hr. ft.^{2} $^\circ$F. In order to examine their conclusion with respect to the present problem, Equation VI-3 may be used. If Nu_c is of the order of 10 to 20, and k_x is assumed to be 10 Btu/hr. ft.^{2} $^\circ$F./ft., the ratio of Nu_c to Nu_o would range from 8.7 to 18.4. Clearly a resistance too small to be measured in the work of Moyer and Riemen would be completely controlling in the studies of heat transfer to sodium in an entrance region.

In sodium wetting tests presented by Winkler and Vandenburg (39), the electrical resistance across the interface was used to indicate the wetting temperature of stainless steel 347, molybdenum, nickel, low carbon steel, and glass. Samples of molybdenum and nickel which had previously been wet by sodium (and washed off) were subsequently wet at the melting point of sodium (208°F). Otherwise, the wetting temperatures ranged from about 284°F to 632°F. Although they made no measurements with copper, it may be significant that the upper limit of operating temperature in the experimental heat transfer system was about 300°F because of the Hycar hard rubber gaskets in the test section.

In his studies involving the mercury-steel interface, Droher (9) used a cylindrical glass cell sealed on each end with the metal surfaces being tested. A fixed current was passed through the cell and the potential was measured at points along the cell so as to indicate the potential drop across each interface. Part of his conclusions which pertain to the present discussion are repeated as follows:

. . . . . .

2. The interfacial electrical resistance is extremely sensitive to surface conditions. This is evident from the extreme difficulty of reproducing results under apparently identical conditions. These anomalies could only be attributed to factors in operation affecting the surface conditions which could not be controlled.

3. The existence of wetting, as defined by low contact angles or retention of a silvery film, is a sufficient but not a necessary condition for low interfacial electrical resistance. It is believed that the thermal-electrical analogy applies to interfacial resistances in an approximate qualitative sense, but not in an exact sense. This same conclusion, probably, then also applies to the interfacial thermal resistance.

4. It is possible to produce surfaces which give low interfacial electrical resistances but do not exhibit wetting in the conventional sense.

. . . . . .

11. Tests on copper specimens always result in zero interfacial electrical resistance, which do not change with time, regardless of whether the surface was amalgamated prior to the test. Stainless steel specimens always result in appreciable values of interfacial electrical resistance.

. . . . . .

The last conclusion is repeated to lend support to the validity of the heat transfer data for mercury in the copper test section. The first conclusions are repeated here to emphasize the uncertainties that exist when a surface is not wetted. Though Droher points out that only qualitative inferences may be drawn about interfacial thermal resistance from electrical resistance measurements, some of his equipment was modified for a brief study of the electrical resistance across the sodium-copper interface. The average of six determinations of the resistance across an interface of approximately 0.56 $in.^2$ area was 6 to 7 micro-ohms. Since Droher pointed out that a low resistance does not necessarily imply good wetting, the results are inconclusive. However, it is rewarding to examine a few of the possibilities for the thermal resistance in question. Consider a case where the computed Nusselt modulus is 20 and the experimentally measured value is 5. Equation VI-3 may be used to compute the thickness of various substances which would give this required additional thermal resistance. Typical figures for a system with 1/16 in. diameter are shown in Table V. Using some rough values for the electrical resistivity, the electrical resistance of a film of thickness x in the conductivity cell is also shown in the table. As indicated in the table, while thermal conductivity varies over a range of 500, the electrical resistivity varies over a range of 10^9. The wide band between iron and the oxides must include numerous other possibilities. The only conclusion which can be drawn is that interfacial electrical resistance measurements are meaningless in the

TABLE V

RELATIVE VALUES OF THERMAL AND ELECTRICAL INTERFACIAL RESISTANCE

Material	k, Btu/hr.ft.^{2} $^\circ$F/ft.	x, in.	ρ, ohm cm	R_x, ohm
Na	48	9.4×10^{-3}	10^{-5}	6.6×10^{-8}
Fe or Ni	34	6.6×10^{-3}	10^{-5}	4.7×10^{-8}
Oxides	2 0.1	3.9×10^{-4} 2.0×10^{-5}	300 to 10^4	5.9×10^{-3} to 3.9
Gas	0.02	3.9×10^{-6}		

present study. There is no apparent contradiction in the thermal and electrical measurements, but, on the other hand, there is no proof that the low and erratic sodium data may be attributed to an oxide film or non-wetted condition. It is to the possibility of non-wetting that the appeal is made in the present case. Since, as it has been shown, the experimental system places so much importance on good contact, the existance of a small additional resistance on the copper surface (which is quite likely) would explain the discrepancies. Proof of the hypothesis is difficult, but the present experimental system may be well suited for the thermal studies since the effects are maximized. It is very likely that a non-flow system or a flow system yielding low heat transfer coefficients would not show these effects which are believed to be due to non-wetting.

CHAPTER VII

CONCLUSIONS AND RECOMMENDATIONS

It is believed that the following contributions are made in the present work:

1. The literature on entrance region heat transfer has been reviewed.
2. An analysis has been presented for the effects of longitudinal conduction on heat transfer to liquid metals in a thermal entrance.
3. An experimental apparatus has been designed and operated for the purpose of obtaining data on entrance region heat transfer to liquid metals. The same type of apparatus may be easily modified to conform to a variety of entrance conditions.
4. Experimental heat transfer data are presented for mercury in turbulent flow in a thermal entrance region. The data were obtained in three different test sections with a precision of about 2%.
5. Experimental heat transfer data to sodium are reported, but, because they are erratic and very low, they are only used to illustrate the probable existence of non-wetting conditions at a copper-sodium interface.

Conclusions which one may draw from this work are:

1. The effect of longitudinal conduction may be neglected in cases of heat transfer to liquid metals in turbulent flow.
2. Experimental heat transfer data obtained with mercury in turbulent flow confirm the predictions of an analytical conduction solution for values of Pe $\frac{D}{L}$ less than 2000 in test sections of $\frac{D}{L} = 1$ and $\frac{D}{L} = 2$. This solution is predicated on the postulates of negligible eddy conduction and velocity obeying the one-seventh power law.
3. For values of Pe $\frac{D}{L}$ greater than 2000, it is clear that the eddy conduction must be included in the analytical solutions if reasonable agreement with the mercury data is desired. For liquids of higher thermal conductivity than mercury, one would expect data to agree with conduction solutions to higher values of Pe $\frac{D}{L}$.
4. Very high values of heat flux or heat transfer coefficient may be achieved with liquid metals in the thermal entrance region. Coefficients as high as 66,300 Btu/hr. ft.^{2} $^\circ$F. were measured in the mercury system and it is believed that much higher coefficients are attainable.

The possibilities for extending the scope of the work are numerous and interesting. One recommendation pointed toward a more complete understanding of the effect of velocity distribution is that the experiment be performed over a much wider range of Reynolds modulus. If data were taken over the range of Re from 1000 to 20,000, any shift in agreement with the conduction solutions could be attributed to the change in velocity profile from parabolic to the turbulent distribution. At very high Re (greater than 200,000) it would be desirable to change the ratio of heated length to diameter so as to fill in the region of uncertainty between "long tube" predictions, which include eddy conduction, and "entrance region" predictions, which do not include eddy conduction. Presumably, there will always be a region very near the entrance to a heated channel, where the thermal boundary layer has not developed beyond the laminar sublayer. In this region, the eddies would be ineffective in the heat transfer mechanism and the solutions for cases with and without eddy conduction should come together.

In the pursuit of a study of the effect of wetting on heat transfer, it is believed that the use of a test section, such as the one described in the present work, offers the advantage of maximizing effects of any surface film or unusual conditions.

Copper was selected for the plate material in the test section because of its high thermal conductivity. It may be possible to find some other material which has a sufficiently high thermal conductivity and which will be wet more readily by sodium. If further studies

involving sodium and copper are pursued, it may be possible to achieve good contact by operating a system at a higher temperature. This will create either a new design problem or a new materials problem, for the Hycar rubber gasket in the present test section eliminates this alternative.

Another alternative appears as a result of the solubility of silver in sodium. It may be feasible to silver plate a copper surface prior to contact with sodium. When the silver dissolves in the sodium, a fresh, unoxidized copper surface will be exposed at the interface.

Although the present emphasis has been directed toward liquid metals, the test section used in this work is equally well suited for use with other heat transfer media. With liquids of lower thermal conductivity than sodium, the wetting problem would be reduced since the interfacial thermal resistance probably would be reduced relative to the total thermal resistance. Even for water and air, there is currently very little information available on heat transfer in entrance regions. The promise of high heat transfer coefficients in entrance regions may also justify some effort to apply these concepts to a practical heat exchanger. Where size of exchanger is a serious limitation and high pumping power can be supplied in return for the saving in space, it may be possible to remove great quantities of heat from a small volume by having a number of parallel, short tubes in a bundle.

It is hoped that the present work will motivate additional investigation in this "entrance region" segment of the field of heat transfer. The academic interest is great and the practical potentialities are manifold.

BIBLIOGRAPHY

BIBLIOGRAPHY

1. Bailey, R. V., Heat Transfer to Fluids of Low Prandtl Modulus in the Entrance Section of a Tube - Uniform Velocity and Temperature at the Entrance, unpublished manuscript at Oak Ridge National Laboratory, August 1951.

2. Baranowski, F., Jury, S. H., unpublished work, Chemical Engineering Department, University of Tennessee

3. Boelter, L.M.K., Cherry, V. H., Johnson, H. A., Martinelli, R. C., Heat Transfer Notes, University of California Press, Berkeley and Los Angeles, 1948.

4. Boelter, L.M.K., Young, G., Iversen, H. W., An Investigation of Aircraft Heaters XXVII - Distribution of Heat-Transfer Rate in the Entrance Section of a Circular Tube, National Advisory Committee for Aeronautics, Technical Note No. 1451, Washington, July 1948.

5. Carslaw, H. S., Jaeger, J. C., Conduction of Heat in Solids, Oxford, 1947.

6. Cholette, A., "Heat Transfer - Local and Average Coefficients for Air Flowing Inside Tubes," Chem. Eng. Prog., 44, 81-88 (1948).

7. The Dowtherm Story, Dow Chemical Company, Midland, Michigan

8. Drew, T. B., "Mathematical Attacks on Forced Convection Problems: A Review," Trans. Am. Inst. Chem. Engrs., 26, 26-80 (1931)

9. Droher, J. J., Studies of Interfacial Effects between Mercury and Steel, M.S. Thesis, Chemical Engineering Department, University of Tennessee, June 1952

10. Dusinberre, G. M., Numerical Analysis of Heat Flow, McGraw-Hill, New York, 1949.

11. English, D., Barrett, T., Heat Transfer Properties of Mercury, A.E.R.E. E/R 547, Ministry of Supply, Harwell, Berks., June 1950.

12. Gehlhoff, G., Neumeier, F., "Thermal Conductivity, Electrical Conductivity, Thermoelectric Force, and Wiedemann-Franz Number of Mercury between -190° and +150°C and Their Variation with Transition from Solid to Liquid State," Ber. deut. phys. Ges., 21, 201-17 (1919).

13. Graetz, L., Annalen der Physik (N.F.) 25, 337-357 (1885).

14. Graetz, L., Annalen der Physik (N. F.) 18, 79-94 (1883)

15. Hall, W. C., "The Thermal Conductivities of Mercury, Sodium, and Sodium Amalgams in the Liquid State," Physical Review, 53, 1004-1009 (1938).

16. Humble, L. V., Lowdermilk, W. H., Grele, M., Heat Transfer from High Temperature Surfaces to Fluids, I-Preliminary Investigation with Air in Inconel Tube with Rounded Entrance, Inside Diameter of 0.4 Inch and Length of 24 Inches, National Advisory Committee for Aeronautics, Research Memorandum No. E7L31, Washington, May 21, 1948.

17. Jakob, M., Heat Transfer, Vol. 1, John Wiley, N. Y., 1949

18. Jenkins, R., "Variation of the Eddy Conductivity with Prandtl Modulus and Its Use in Prediction of Turbulent Heat Transfer Coefficients," 1951 Heat Transfer and Fluid Mechanics Institute, Stanford University Press, Stanford, California, p.147-158.

19. Jenkins, R., Brough, H. W., Sage, B. H., "Prediction of Temperature Distribution in Turbulent Flow," Ind. Eng. Chem., 43, 2483-2486 (1951).

20. Johnson, H. A., Hartnett, J. P., Clabaugh, W. J., "Heat Transfer to Molten Lead-Bismuth Eutectic in Turbulent Pipe Flow," 1952 Heat Transfer and Fluid Mechanics Institute, Stanford University Press, Stanford, California, p.5-18.

21. Latzko, H., "Der Warmeubergang an einen turbulenten Flussigkeit oder Gasstrom," Zeitschrift fur angewandte Mathematik und Physik, 1, No. 4, August 1921 (translated by National Advisory Committee for Aeronautics, Technical Memorandum No. 1068).

22. Lee, A., Nelson, W. O., Cherry, V. H., Boelter, L.M.K., Proc. 5th Internat. Congress Appl. Mech., 571 (1938).

23. Leveque, M. A., "Transmission de Chaleur par Convection," Annales des Mines (12), 13, 201, 305, 381 (1928).

24. Liquid Metals Handbook, Lyon, R. N., Ed., 1st Ed., Atomic Energy Commission - Department of the Navy, June 1950 (2nd. Ed. 1952)

25. Lyon, R. N., Forced Convection Heat Transfer Theory and Experiments with Liquid Metals, ORNL-361, Oak Ridge National Laboratory, August 1949.

26. McAdams, W. H., Heat Transmission, 2nd Ed., McGraw-Hill, N. Y., 1942

27. Martinelli, R. C., "Heat Transfer to Molten Metals," Trans. Am. Soc. Mech. Engrs., 69, 947-959 (1947)

28. Moyer, J. W., Riemen, W. A., Heat Transfer Measurements at Sodium-Stainless Steel Interface, KAPL-567, Knolls Atomic Power Laboratory, June 1, 1951.

29. Perry, R. L., Berggren, W. P., "Transient Heat Conduction in Hollow Cylinders after Sudden Change of Inner Surface Temperature," University of California Publications in Engineering, 5, 59 (1944).

30. Poppendiek, H. F., Forced Convection Heat Transfer in Thermal Entrance Regions, Part I, ORNL-913, Oak Ridge National Laboratory, March 1951.

31. Poppendiek, H. F., Palmer, L. D., Forced Convection Heat Transfer in Thermal Entrance Regions, Part II, ORNL-914, Oak Ridge National Laboratory, May 1952.

32. Prandtl, L., Tietjens, O. G., Applied Hydro- and Aeromechanics, McGraw-Hill, New York, 1944.

33. Sanders, V. D., A Mathematical Analysis of the Turbulent Heat Transfer in a Pipe with a Surface Temperature Discontinuity at Entrance, M.S. Thesis, University of California, November 1946.

34. Scarborough, J. B., Numerical Mathematical Analysis, Johns Hopkins Press, Baltimore, 1950.

35. Schlichting, H., Lecture Series "Boundary Layer Theory," Part II - Turbulent Flows, National Advisory Committee for Aeronautics, Technical Memorandum No. 1218, Washington, April 1949.

36. Seban, R. A., Shimazaki, T., Heat Transfer to a Fluid Flowing Turbulently in a Smooth Pipe with Walls at Constant Temperature, Paper No. 50-A-128 presented at Annual Meeting, Am. Soc. Mech. Engrs, New York, 1950.

37. Seban, R. A., Shimazaki, T., Calculations Relative to the Thermal Entry Length for Fluids of Low Prandtl Number, University of California, January 1950.

38. Sherwood, T. K., Reed, C. E., Applied Mathematics in Chemical Engineering, McGraw-Hill, New York, 1939.

39. Winkler, H. H., Vandenburg, L. B., Method and Results of Sodium Wetting Tests, KAPL-P-231, Knolls Atomic Power Laboratory, December 27, 1949.

APPENDIX

APPENDIX A

CONDUCTION SOLUTION FOR PARABOLIC VELOCITY DISTRIBUTION

Jakob (17) and Boelter et al (3) present complete discussions of the solution of Graetz (13) for laminar flow through a tube having uniform wall temperature. The local heat transfer coefficient may be defined according to the equation

$$h_x = \frac{k \frac{\partial t}{\partial y}(x,0)}{(t_m - t_w)} \qquad \text{A-1}$$

Values for $k\frac{\partial t}{\partial y}(x,0)$ and $(t_m - t_w)$ are taken from Jakob as follows:

$$k\frac{\partial t}{\partial y}(x,0) = k\frac{t_o - t_w}{b}\left[1.499e^{-m_0 x} + 1.078e^{-m_1 x} + 0.358e^{-m_2 x} + \cdots\right] \qquad \text{A-2}$$

$$t_m - t_w = (t_o - t_w)\left[0.820e^{-m_0 x} + 0.0972e^{-m_1 x} + 0.0135^{-m_2 x} + \cdots\right] \qquad \text{A-3}$$

where t_o is the initial fluid temperature, t_w is the wall temperature, and the exponentials may be rearranged so that $m_n x = \frac{2\gamma_n^2}{Re\,D}x$

Values of γ_n are given as follows:

$$\gamma_0 = 2.705, \quad \gamma_1 = 6.66, \quad \gamma_2 = 10.3, \quad \gamma_3 = (14.67)$$

The value for γ_3 is indicated by Jakob in a footnote (p.453) referring to work of Lee, Nelson, Cherry, and Boelter (22).

Equations A-2 and A-3 may be combined to give

$$Nu_x = 2\frac{\left[1.499e^{-\frac{2(2.705)^2}{Pe\frac{D}{x}}} + 1.078e^{-\frac{2(6.66)^2}{Pe\frac{D}{x}}} + 0.358e^{-\frac{2(10.3)^2}{Pe\frac{D}{x}}} + ---\right]}{\left[0.820e^{-\frac{2(2.705)^2}{Pe\frac{D}{x}}} + 0.0972e^{-\frac{2(6.66)^2}{Pe\frac{D}{x}}} + 0.0135e^{-\frac{2(10.3)^2}{Pe\frac{D}{x}}} + --\right]} \quad \text{A-4}$$

In order to obtain the average values of Nusselt Modulus between the entrance and x = L, a new definition may be made as follows:

Let $$\Psi = \left[0.820e^{-\frac{2(2.705)^2}{Pe\frac{D}{x}}} + 0.0972e^{-\frac{2(6.66)^2}{Pe\frac{D}{x}}} + 0.0135e^{-\frac{2(10.3)^2}{Pe\frac{D}{x}}} + --\right] \quad \text{A-5}$$

$$d\Psi = -\frac{8}{Pe}\left[1.499e^{-\frac{2(2.705)^2}{Pe\frac{D}{x}}} + 1.078e^{-\frac{2(6.66)^2}{Pe\frac{D}{x}}} + 0.358e^{-\frac{2(10.3)^2}{Pe\frac{D}{x}}} + -\right] \quad \text{A-6}$$

Thus

$$Nu_L = \frac{D}{L}\int_0^{\frac{L}{D}} Nu_x\, d\left(\frac{x}{D}\right) = -\frac{1}{4}Pe\frac{D}{L}\int_{\Psi(0)}^{\Psi\left(\frac{L}{D}\right)} \frac{d\Psi}{\Psi} \quad \text{A-7}$$

$$Nu_L = -\frac{1}{4}Pe\frac{D}{L}\ln\frac{\left[0.820e^{-\frac{2(2.705)^2}{Pe\frac{D}{L}}} + 0.0972e^{-\frac{2(6.66)^2}{Pe\frac{D}{L}}} + 0.0135e^{-\frac{2(10.3)^2}{Pe\frac{D}{L}}} + --\right]}{\left[0.820 \quad +0.0972 \quad +0.0135 \quad +--\right]} \quad \text{A-8}$$

It can be shown that the sum in the denominator of Equation A-8 is unity, giving Equation A-9 as follows:

$$Nu_L = -\frac{1}{4} Pe \frac{D}{L} \ln \left[0.820 e^{-\frac{2(2.703)^2}{Pe\frac{D}{L}}} + 0.0972 e^{-\frac{2(6.66)^2}{Pe\frac{D}{L}}} + 0.0135 e^{-\frac{2(10.3)^2}{Pe\frac{D}{L}}} + \cdots \right] \quad \text{A-9}$$

Values of Nu_x and Nu_L are shown in Table VI.

TABLE VI

COMPUTED VALUES OF NUSSELT MODULI FOR PARABOLIC VELOCITY DISTRIBUTION

$Pe\,\frac{D}{x}$, $Pe\,\frac{D}{L}$	Nu_x	Nu_L
1	3.65	3.69
10	3.66	4.15
40	4.00	5.48
100	4.76	7.14

APPENDIX B

AVERAGE NUSSELT MODULI FOR THE UNIFORM VELOCITY CASE

In the body of the report[1], an equation was presented as the solution for local Nusselt moduli in circular tubes. This was for the case of uniform velocity in a thermal entrance region of uniform wall temperature.

$$Nu_x = \frac{\sum_{n=1}^{\infty} e^{-\frac{4\alpha_n^2}{Pe\frac{D}{x}}}}{\sum_{n=1}^{\infty} \frac{1}{\alpha_n^2} e^{-\frac{4\alpha_n^2}{Pe\frac{D}{x}}}} \qquad \text{B-1}$$

In order to determine average values of Nusselt modulus between the entrance and x = L, a new definition may be made as follows:

Let $$\Omega = \sum_{n=1}^{\infty} \frac{1}{\alpha_n^2} e^{-\frac{4\alpha_n^2}{Pe\frac{D}{x}}} \qquad \text{B-2}$$

$$\frac{d\Omega}{d(\frac{x}{D})} = \sum_{n=1}^{\infty} -\frac{4}{Pe} e^{-\frac{4\alpha_n^2}{Pe\frac{D}{x}}} \qquad \text{B-3}$$

Then $$Nu_x = -\frac{Pe}{4}\frac{d\Omega}{\Omega} \qquad \text{B-4}$$

---

1. Equations II-10 and III-6

$$Nu_L = \frac{D}{L}\int_0^{\frac{L}{D}} Nu_x \, d\left(\frac{X}{D}\right) = -\frac{1}{4} Pe \frac{D}{L}\int_{\Omega(0)}^{\Omega(\frac{L}{D})} \frac{d\Omega}{\Omega} \qquad \text{B-5}$$

or

$$Nu_L = \frac{1}{4} Pe \frac{D}{L} \ln \frac{\sum_{n=1}^{\infty} \frac{1}{\alpha_n^2}}{\sum_{n=1}^{\infty} \frac{1}{\alpha_n^2} e^{-\frac{4\alpha_n^2}{Pe\frac{D}{L}}}} \qquad \text{B-6}$$

It can be shown that $\sum_{n=1}^{\infty} \frac{1}{\alpha_n^2} = \frac{1}{4}$, leading to Equation B-7

$$Nu_L = -\frac{1}{4} Pe \frac{D}{L} \ln 4 \sum_{n=1}^{\infty} \frac{1}{\alpha_n^2} e^{-\frac{4\alpha_n^2}{Pe\frac{D}{L}}} \qquad \text{B-7}$$

Some local and average values of the Nusselt modulus are shown in Table VII.

TABLE VII

COMPUTED VALUES OF NUSSELT MODULI FOR UNIFORM VELOCITY DISTRIBUTION

$Pe\,\frac{D}{x}$, $Pe\,\frac{D}{L}$	Nu_x	Nu_L
1	5.78	5.91
4	5.78	6.14
10	5.78	6.71
40	6.17	9.30
100	7.74	13.2
400	13.08	24.3
1000	19.50	37.2

APPENDIX C

SAMPLE CALCULATIONS

Mercury Run No. 6

Plate thickness, L = 0.124 in.

Hole diameter, D = 0.125 in.

Mercury temperatures (copper constantan couples)

upstream from test section - 0.879 m.v., 72.1°F

downstream from test section - 0.979 m.v., 76.2°F

According to Equation V-2

$$t = t_w + \frac{q}{2\pi kL} \ln \frac{r}{b}$$

The value of b in this case is D/2 = 1/16"

The plot of t versus log $\frac{r}{b}$ is shown on Figure 11.

From this plot, the value of the slope is determined as S = 179.3 - 127.3 = 52.0 where 179.3 and 127.3 correspond to $\frac{r}{b}$ of 10 and 1, respectively. The value of the heat rate, q, may be computed from the slope as follows:

$$S = \frac{2.303\, q}{2\pi kL} = 52.0\ ^{\circ}F.$$

$$q = \frac{(52.0)(2\pi kL)}{2.303} = \frac{(52.0)(2)(\pi)(220)(0.124)}{(2.303)(12)} = 323 \text{ Btu/hr.}$$

The heat transfer area is A = 2πrL or πDL ft.^{2}

$$A = \pi DL = \frac{\pi(0.125)(0.124)}{144} = 3.39 \times 10^{-4} \text{ ft.}^2$$

TABLE VIII

TEMPERATURE DISTRIBUTION IN TEST SECTION PLATE
(COPPER CONSTANTAN COUPLES)

Thermocouple	r, in.	Emf, millivolts	t., ^{o}F
1	1/4	2.923	158.6
2	1/4	2.923	158.6
3	1/2	5.311	174.2
4	1/2	3.304	173.9
5	7/8	3.642	187.3
6	7/8	3.626	186.6
7	1 1/4	3.831	194.7
8	1 1/4	3.831	194.7

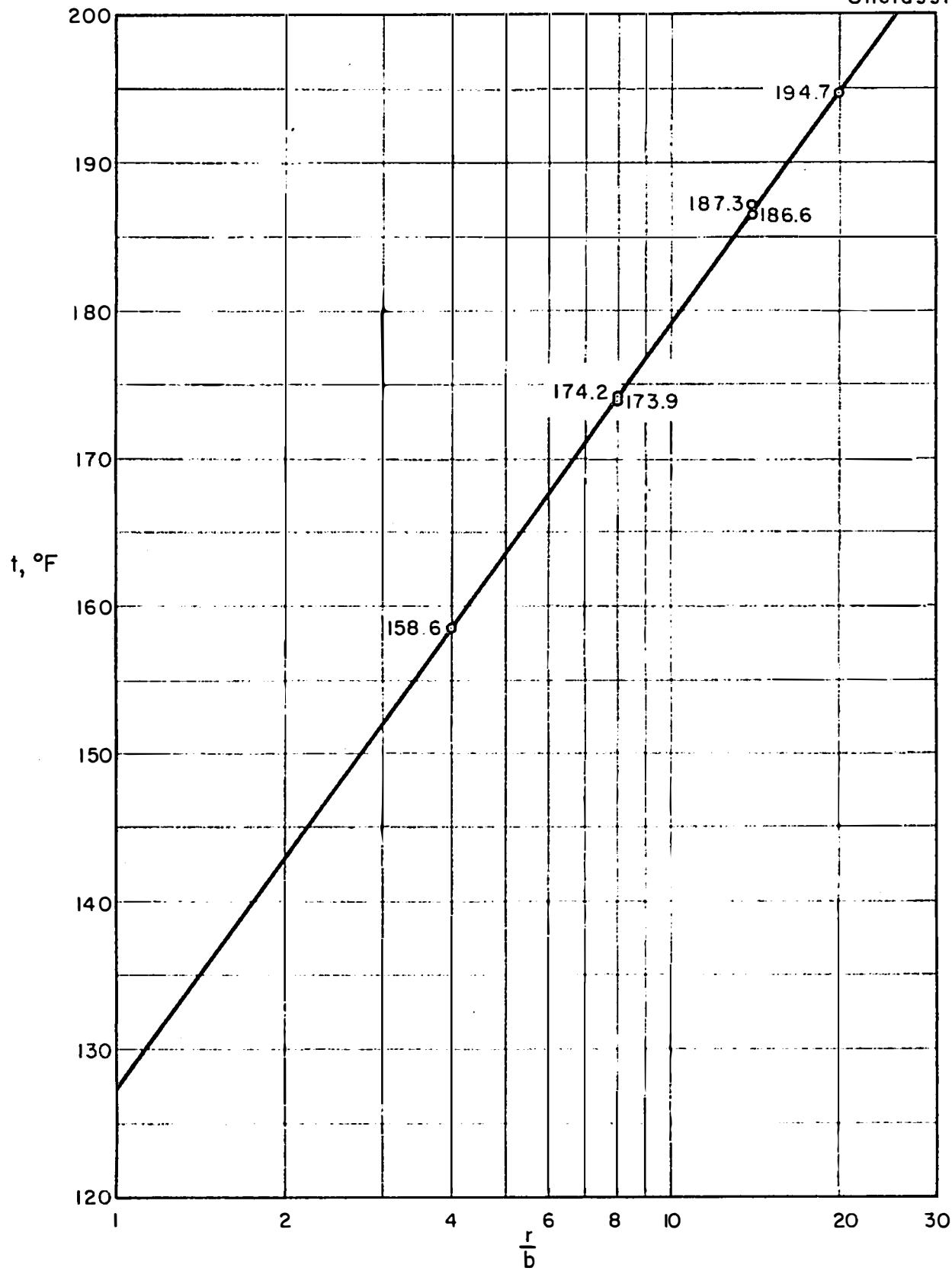

Fig. 11. Temperature Distribution in Test Section Plate for Run 6.

From Figure 11, t_w is found to be 127.3 °F. The mean mercury temperature is 74.2°F.

Then

$$(t_w - t_m) = 127.3 - 74.2 = 53.1\ ^{o}F.$$

The heat transfer coefficient, h, is computed as follows:

$$h_L = \frac{q}{A(t_w - t_m)} = \frac{323}{(3.39 \times 10^{-4})(53.1)} = 17950 \text{ Btu/hr. } \frac{\text{ft.}^2}{^{o}\text{F.}}$$

$$Nu_L = \frac{h_L D}{k} = \frac{(17950)(0.125)}{(5.10)(12)} = 36.7$$

(Thermal conductivity data of Hall are used in this example)

The Reynolds modulus is frequently written as $\frac{DU\rho}{\mu}$ but it may also be expressed as $\frac{4W}{\pi \mu D}$ where W is weight flow rate in lb./hr. The catch tank holds 8.18 lb. of mercury between probes. The time required to fill the tank in this run was 15.25 seconds.

$$Re = \frac{4W}{\pi \mu D} = \frac{(4)\ \frac{8.18 \times 3600}{15.25}}{\pi\ (3.65)\ \frac{0.125}{12}} = 64600$$

Prandtl modulus (based on thermal conductivity data of Hall) is 0.0241

Thus Pe and Pe $\frac{D}{L}$ (since $\frac{D}{L} = 1.0$) are both equal to

$$Pe\ \frac{D}{L} = Re \cdot Pr \cdot \frac{D}{L} = (64600)(0.0241)(1.0) = 1560$$

APPENDIX D

PHYSICAL PROPERTIES OF MERCURY AND SODIUM

Physical properties of mercury and sodium are shown on Figure 12. The values shown are interpolated from data tabulated in the Liquid-Metals Handbook (24). For mercury, thermal conductivity data of Gehlhoff and Neumeier (12) appeared in the first edition, but the data of Hall (15) are included in the second edition. The data of Hall are considered to be more reliable.

Unclassified

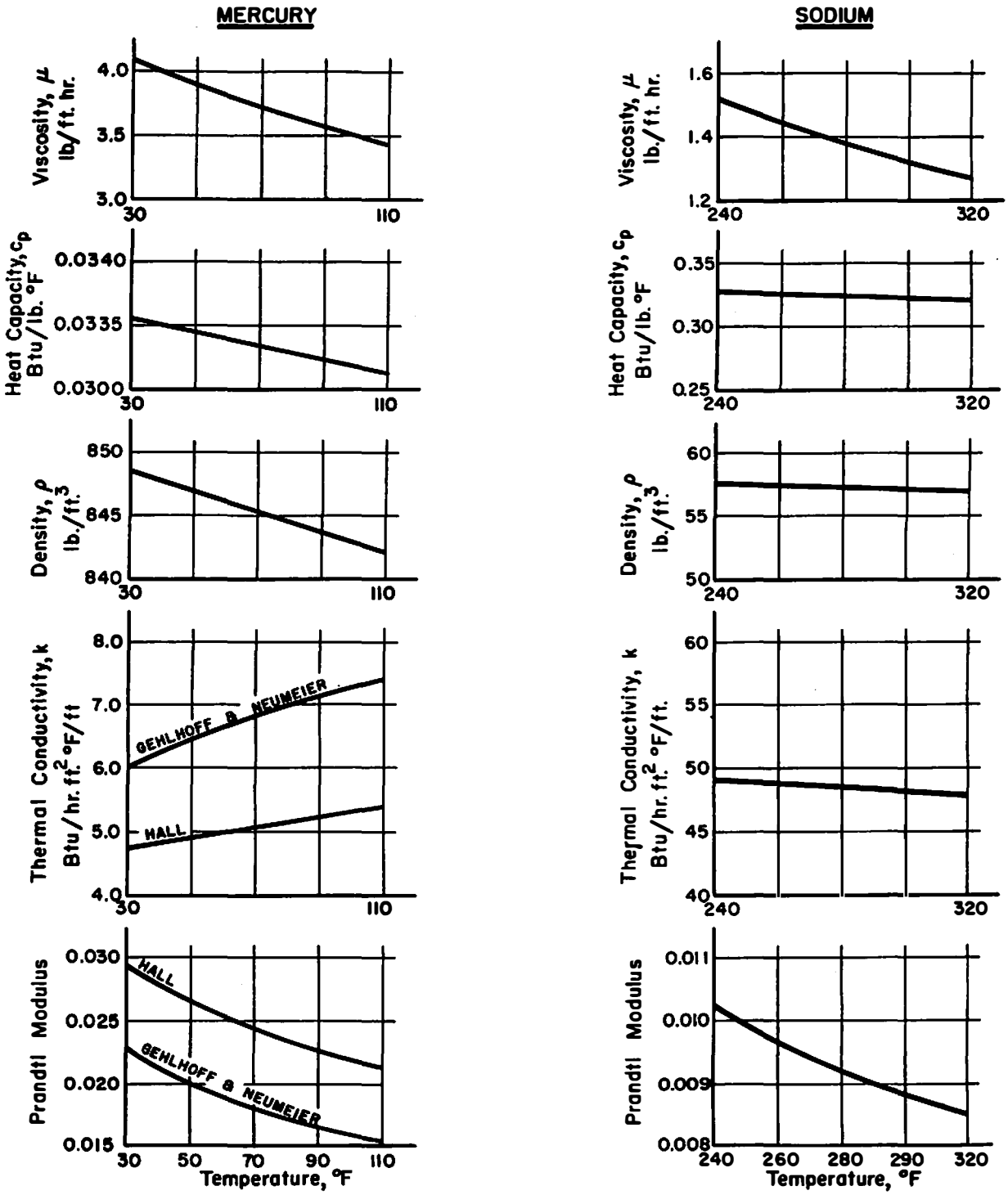

Fig. 12. Physical Properties of Mercury and Sodium

APPENDIX E

ANALYSIS OF HEAT LOSS THROUGH TEST SECTION GASKET

In the evaluation of how closely the experimental heat transfer system compares with the ideal system, it was necessary to estimate the amount of heat conducted across the corner of the hard rubber gasket shown on Figure 5. An idealization of this conduction problem is as follows. Consider the finite hollow cylinder shown on Figure 13a. The problem is to determine the amount of heat conducted from the face in contact with the test plate, $x = 0$, to the fluid through surface $r = a$. Consider the surfaces $r = b$ and $x = L$ to be insulated. Since the system is symmetrical about the x axis, it is necessary to study the temperature distribution in only half of the cross-section. The analytical solutions of several similar problems of steady conduction in finite hollow cylinders are presented by Carslaw and Jaeger (5). Since the form of these analytical solutions is cumbersome and the present problem does not demand great precision, a relaxation method was selected for the present study. Application of the relaxation procedure to many heat transfer problems has been treated by Dusinberre (10), Scarborough (34) and Jakob (17), but a superficial review of their work revealed no information on how best to apply the method to the two-dimensional case in cylindrical coordinates. Consequently, a procedure has been improvised for selecting radial increments so that the usual relaxation process may be applied as if the geometry consisted of a rectangular coordinate network.

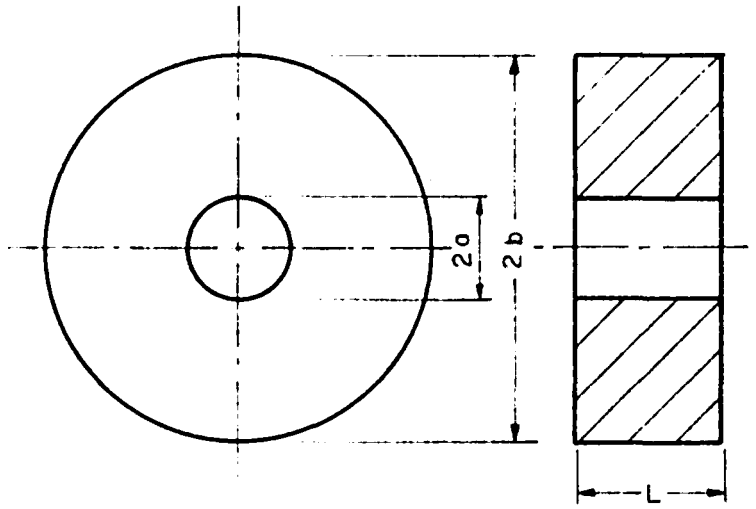

(a.)

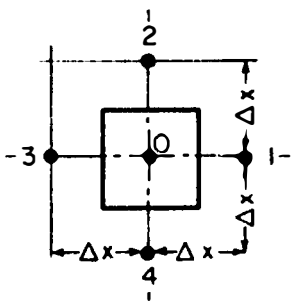

(b.)

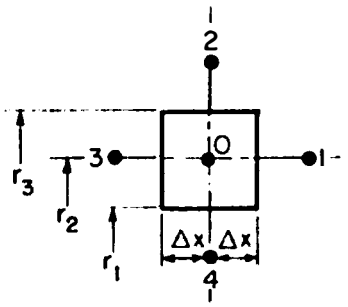

(c.)

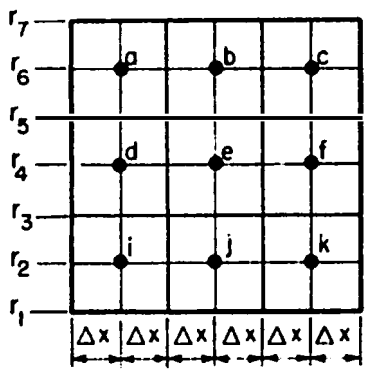

(d.)

Fig. 13. Network for Gasket Analysis.

In the two-dimensional rectangular coordinate network, it is common to arrange reference units with equal heat transfer areas parallel to the coordinate axes. A heat balance over the unit indicated on Figure 13b is

$$q_o = k\left[\frac{A_1}{\Delta X_1}(t_1 - t_o) + \frac{A_2}{\Delta X_2}(t_2 - t_o) + \frac{A_3}{\Delta X_3}(t_3 - t_o) + \frac{A_4}{\Delta X_4}(t_4 - t_o)\right] \qquad \text{E-1}$$

$$\text{If } \frac{A_1}{\Delta X_1} = \frac{A_2}{\Delta X_2} = \frac{A_3}{\Delta X_3} = \frac{A_4}{\Delta X_4} \text{ then } q_o = \frac{kA}{\Delta X}\left[t_1 + t_2 + t_3 + t_4 - 4t_o\right] \qquad \text{E-2}$$

It is usually on this basis that the relaxation procedure is applied to the two-dimensional problems in rectangular coordinates. Now consider a similar heat balance for a unit in the cylindrical coordinate network shown on Figure 13c. If temperature at each edge is the arithmetic average of the center temperatures of the adjoining units, one obtains

$$q_o = \pi k\left[\frac{(r_3^2 - r_1^2)}{2\Delta X}(t_1 - t_o) + \frac{2\Delta X}{\ln \frac{r_3}{r_2}}(t_2 - t_o) + \frac{(r_3^2 - r_1^2)}{2\Delta X}(t_3 - t_o) + \frac{2\Delta X}{\ln \frac{r_3}{r_1}}(t_4 - t_o)\right] \qquad \text{E-3}$$

(The validity of this choice of edge temperature is examined later.) Thus, the only conditions for which the temperature term is analogous to the rectangular geometry are:

$$(1)\ \frac{r_2}{r_1} = \frac{r_3}{r_2} \qquad \text{and (2)} \qquad \frac{r_3^2 - r_1^2}{2\Delta X} = \frac{2\Delta X}{\ln \frac{r_3}{r_2}}$$

where the Equation E-3 becomes

$$q_o = \frac{\pi k(r_3^2 - r_1^2)}{2\Delta x}\left[t_1 + t_2 + t_3 + t_4 - 4t_o\right] \qquad \text{E-4}$$

These conditions may be written as follows

$$4\Delta x^2 = (r_3^2 - r_1^2)\ln\frac{r_3}{r_2} = r_1^2\left[\frac{r_3^2}{r_1^2} - 1\right]\ln\frac{r_3}{r_1}$$

If $$P = \frac{r_3}{r_1} = \frac{r_3}{r_2}\cdot\frac{r_2}{r_1} = \left(\frac{r_3}{r_2}\right)^2$$

then $$8\Delta x^2 = r_1^2(P-1)\ln P$$

With a network covering the section shown on Figure 13d, it is desirable to keep the value of Δx fixed for all units of the network. Similarly to the equations set up above, one may also show that

$$8\Delta x^2 = r_3^2(Q^2-1)\ln Q \quad \text{where} \quad Q = \frac{r_3}{r_8}$$

and

$$8\Delta x^2 = r_5^2(R^2-1)\ln R \quad \text{where} \quad R = \frac{r_3}{r_5}$$

Clearly, this may be continued for any number of additional radial increments.

Letting $r_7 = b$ and $r_1 = a$, one obtains the following equations -

$$a^2(P^2-1)\ln P = r_3^2(Q^2-1)\ln Q = r_5^2(R^2-1)\ln R$$

which may be rearranged to get

$$\frac{1}{P^2}(P^2-1)\ln P = (Q^2-1)\ln Q \quad \text{and} \quad \frac{1}{Q^2}(Q^2-1)\ln Q = (R^2-1)\ln R$$

This procedure is also general for any number of additional radial increments. The relation which ties these factors to a specific case is that the product, P•Q•R , must equal the ratio of outside radius to inside radius, b/a. Although the procedure is essentially one of trial and error, it is simple and may be performed quickly. The functions $(M^2-1) \ln M$ and $\frac{1}{M^2}(M^2-1) \ln M$ are plotted on Figure 14 for various values of M. In order to illustrate the procedure, consider the network shown on Figure 13d. Three regions are indicated radially, so it is necessary to determine values of P, Q, and R to conform to the relations noted above. For the first trial, let P = 1.8. From Figure 14, it is seen that if P = 1.8, then Q = 1.45. But if Q = 1.45, then R = 1.31. The product PQR is 3.42. In the present case, it is found that P = 2.0, Q = 1.505, R = 1.336 gives a product of 4.02 which compares favorably with b/a = 4 for the present system. The radial increments for the present analysis may now be determined as follows:

$r_1 = a = \frac{1}{16}$ in. = 0.0625 $\qquad r_1^2 = 0.00391$

$r_3 = 2r_1 = \frac{1}{8}$ in. = 0.125 $\qquad r_3^2 = 0.0156$

$r_5 = 1.5r_3 = \frac{3}{16}$ in. = 0.1875 $\qquad r_5^2 = 0.0352$

$r_7 = b = 1.33\ r_5 = \frac{1}{4}$ in. = 0.250 $\qquad r_7^2 = 0.0625$

$$\frac{\Delta x^2}{r_1^2} = \frac{(P^2-1)}{8} \ln P = \frac{(4-1)}{8} \ln 2.0 \approx 0.26$$

$$\Delta x = 0.51 r_1 = 0.0319$$

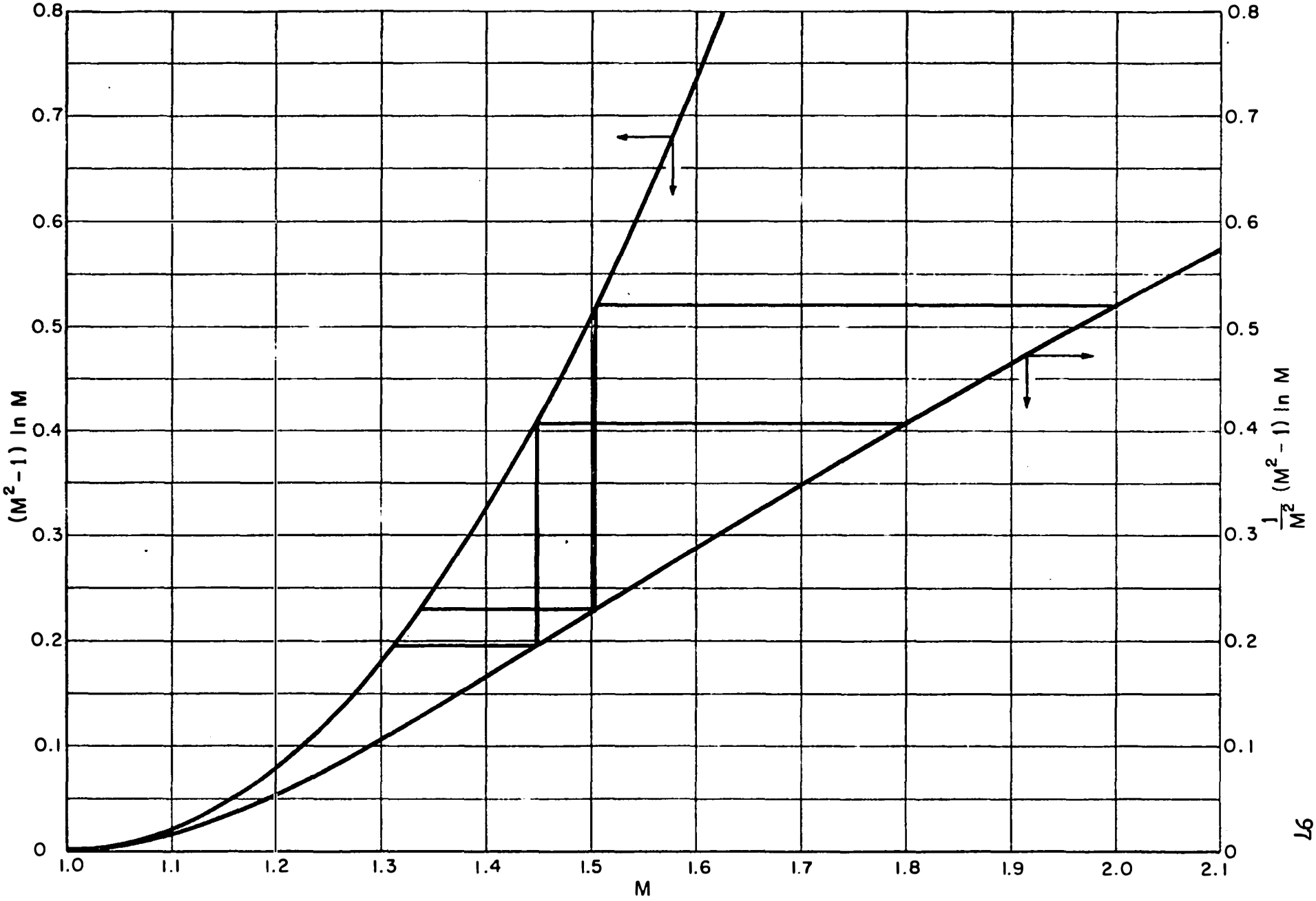

Fig. 14 Functions for Use in Gasket Analysis

It is now possible to consider the validity of the choice of edge temperature as the arithmetic average of the temperatures characterizing two adjacent units of the network. In case of unidirectional radial heat flow in a cylinder of the dimensions shown above, the temperature distribution would be described by the equation

$$t - t_a = \frac{q}{2\pi k L} \ln \frac{r}{a}$$

Letting $t_b - t_a = 100^{\circ}F$, it is found that $\frac{q}{2\pi kL} = \frac{100}{\ln 4}$

Thus $t - t_a = \frac{100}{\ln 4} \ln \frac{r}{a}$

Values of t at different radial positions are shown on Table IX. For the case studied, it appears that the choice of edge temperature is adequate, on the basis of the close approximation of the average temperatures to the computed value for unidirectional radial heat flow.

It is necessary to make special considerations for units which are oriented at borders of the network. Consider a corner such as unit "i" of Figure 13d. The heat balance may be made as follows:

$$q_{o,i} = \pi k \left[\frac{(r_3^2 - r_1^2)}{2\Delta x}(t_1 - t_o) + \frac{2\Delta x}{\ln \frac{r_3}{r_2}}(t_2 - t_o) + \frac{(r_3^2 - r_1^2)}{2\Delta x}(2t_{r_2,0} - 2t_o) + \frac{2\Delta x}{\ln \frac{r_3}{r_1}}(2t_{a,\Delta x} - 2t_o) \right] \qquad \text{E-5}$$

where $t_{r_2,0}$ refers to the temperature at radius r_2 along the plane $x = 0$ and $t_{a,\Delta x}$ refers to the temperature at $r = a$ and $x = \Delta x$. For Equation E-5 to be analogous to Equations E-2 and E-4, it may be written as follows:

TABLE IX

RADIAL TEMPERATURE DISTRIBUTION IN A CYLINDER

r	$\frac{r}{a}$	$\ln \frac{r}{a}$	$t-t_a$	$t_{r_m}-t_a = \frac{t_{r_{m-1}} + t_{r_{m+1}}}{2}$
r_1	1	0	0	
r_2	$\sqrt{2}$	0.3464	24.99	25.00
r_3	2	0.6932	50.01	
r_4	$2\sqrt{1.5}$	0.8961	64.65	64.65
r_5	3	1.099	79.29	
r_6	$3\sqrt{1.33}$	1.241	89.54	89.65
r_7	4	1.386	100.00	

$$q_{o_i} = \frac{2\Delta x}{\ln D}\,\pi k\left[t_1 + t_2 + 2t_{r,0} + 2t_{a,\Delta x} - 6t_o\right] \qquad \text{E-6}$$

A work sheet is shown on Figure 15. The numbers in the circles are proportional to the change in q_o for each unit of the network, corresponding to a temperature change at t_o of one degree. (This is the number by which t_o is multiplied in the bracketed temperature term of Equation E-6). Numbers below and to the right are the temperatures at the circled points, and numbers below and to the left are the corresponding values proportional to q_o. The numbers shown on Figure 15 represent the temperature field resulting from the boundary conditions $t(r,0) = 100$, $t(a,x) = 0$, $\frac{\partial t}{\partial r}(b,x) = 0$, and $\frac{\partial t}{\partial x}(r,L) = 0$. One may now compute the rate of heat conduction through the gasket as follows:

$r_7^2 - r_5^2 = 0.0273$ in.^{2}

$r_5^2 - r_3^2 = 0.0195$ in.^{2}

$r_3^2 - r_1^2 = 0.0117$ in.^{2}

$$q_{x=0} = \frac{\pi k}{\Delta x}\left[\frac{(r_7^2 - r_5^2)}{12}(100-84) + \frac{(r_5^2 - r_3^2)}{12}(100-77) + \frac{(r_3^2 - r_1^2)}{12}(100-50)\right]$$

$$= \frac{\pi k}{12\,\Delta x}\left[0.437 + 0.449 + 0.585\right] = 3.84\,\pi k$$

$$q_{r=a} = \frac{4\Delta x\,\pi k}{\ln \frac{r_2}{r_1}}\left[50 + 23 + 16\right] = \frac{4(0.0319)(91)\,\pi k}{12 \ln \sqrt{2}} = 2.79\,\pi k$$

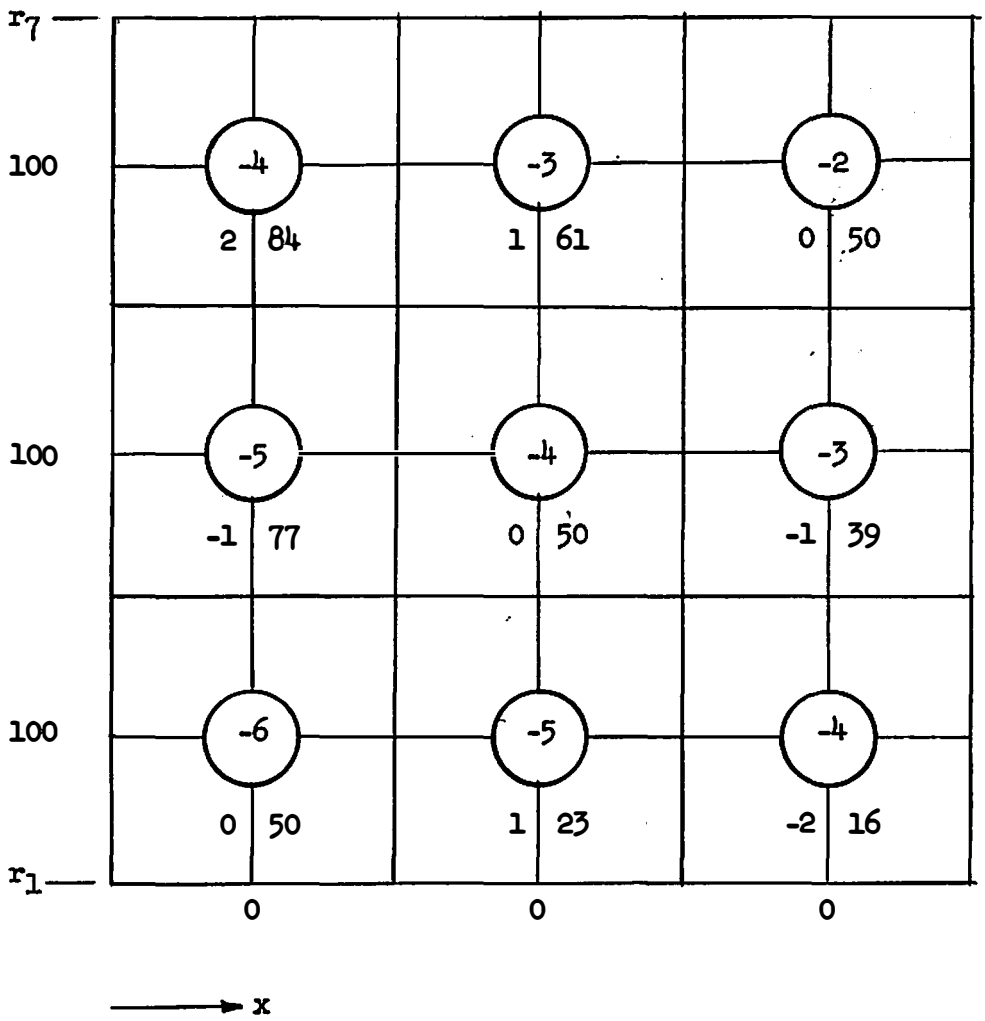

FIG. 15 TEMPERATURE DISTRIBUTION IN GASKET

Clearly, $q_{r=a}$ and $q_{x=0}$ should be equal since the other two possible paths for heat flow are insulated. A network of smaller subdivisions would be expected to bring these values closer together. For the present purposes, the average value will be considered sufficient, i.e., $q = \frac{3.84 + 2.79}{2} \pi k = 3.32 \pi k$ Btu/hr.

If one compares the real and ideal gasket problems, it is seen that the ideal problem has boundary conditions which would lead to greater heat conduction through the gasket than the real problem. For example, the maximum difference between t(b,0) and the fluid temperature is less than 100°F. Furthermore, in the real system, the value of t(a,0) is less than t(b,0) according to an exponential function of radius. If t(a,x) is postulated to be the mean fluid temperature, this implies that the interfacial thermal resistance is zero at r=a. The result is that the driving force is greater and the resistance less in the idealization than in the real case.

If a value k = 0.1 Btu/hr.ft.^{2}($^{\circ}$F/ft) is assumed for the hard rubber, the heat leak is of the order of 1.0 Btu/hr which constitutes less than 1% of the heat flow in the test plate.

APPENDIX F

ESTIMATE OF WALL TEMPERATURE IN THE TEST SECTION

In order to determine the applicability of the postulate of uniform wall temperature to the present experimental system, an iterative procedure (34) has been used to estimate the actual wall temperature distribution in the copper plate.

Consider a geometric network in the copper plate as shown on Figure 16. A heat balance in the network unit designated as (r_2, x_1) may be written as follows:

$$q(r_2,x_1) = \pi k \left[\frac{(r_3^2 - r_1^2)}{\Delta x}(t_1 - t_0) + \frac{2\Delta x}{\ln \frac{r_3}{r_2}}(t_2 - t_0) + \frac{(r_3^2 - r_1^2)}{\Delta x}(t_3 - t_0) + \frac{2\Delta x}{\ln \frac{r_1}{r_0}}(t_4 - t_0) \right] \qquad \text{F-1}$$

Equation F-1 may be rearranged to get

$$q(r_2,x_1) = \frac{2\pi k \Delta x}{\ln P} \left[r_2^2 N(t_1 + t_3 - 2t_0) + (t_2 + t_4 - 2t_0) \right] \qquad \text{F-2}$$

where $N = \dfrac{(P^2-1)\ln P}{2P\Delta x^2}$ $\qquad$ $P = \left(\dfrac{r_1}{r_0}\right)^2 = \left(\dfrac{r_2}{r_1}\right)^2 = \cdots = \left(\dfrac{r_n}{r_{n-1}}\right)^2$

Since, at steady state conditions, $q(r_2,x_1) = 0$, the term in the brackets may be set equal to zero and the resulting expression for t_0 is

$$t_0 = \frac{r_2^2 N(t_1 + t_3) + t_2 + t_4}{2(r_2 N + 1)} \qquad \text{F-3}$$

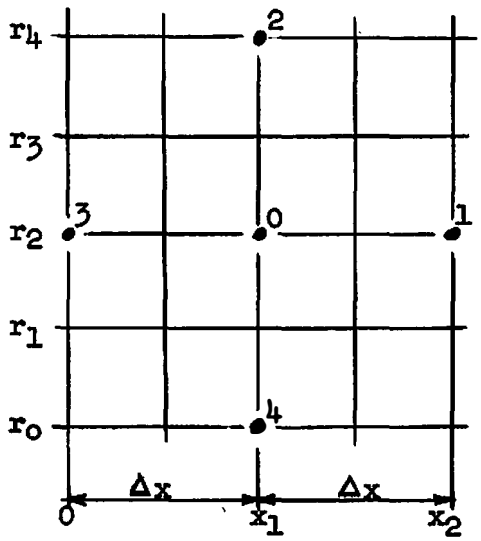

FIG. 16 NETWORK FOR TEST SECTION ANALYSIS

For the case in which $r = r_o$ defines the heat transfer surface, one may write

$$q(r_o, x_1) = \pi k \left[\frac{(r_1^2 - r_o^2)}{\Delta x}(t_1 - t_o) + \frac{2\Delta x}{\ln \frac{r_1}{r_o}}(t_2 - t_o) + \frac{(r_1^2 - r_o^2)}{\Delta x}(t_3 - t_o) + \frac{h(2r_o\Delta x)}{k}(t_m - t_o) \right] \qquad \text{F-4}$$

where t_m is the mean fluid temperature. Thus,

$$t_o = \frac{\frac{r_o^2(P-1)\ln P}{2\Delta x^2}(t_1 + t_3) + t_2}{\frac{r_o^2(P-1)\ln P}{\Delta x^2} + 1 + \frac{hr_o}{k}\ln P} \qquad \text{F-5}$$

where t_m has been set equal to zero. Similar equations may be set up for any particular unit in the geometric network.

As shown in Equations F-4 and F-5, it is necessary to use values of the heat transfer coefficient which correspond to particular locations at the heat transfer surface. Since Equation II-16 may be used to compute average values of the heat transfer coefficient between x = 0 and x = L, it is possible to obtain average values for each increment Δx of L as follows:

$$h_1 = \frac{1}{\Delta x}\int_0^{x_1} h_x \, dx \qquad \text{F-6}$$

$$h_2 = \frac{1}{2\Delta x}\int_0^{x_2} h_x \, dx \qquad \text{F-7}$$

$$h_3 = \frac{1}{3\Delta x}\int_0^{x_3} h_x \, dx \qquad \text{F-8}$$

But

$$h_2 = \frac{1}{2\Delta x}\left[\int_0^{x_1} h_x\,dx + \int_{x_1}^{x_2} h_x\,dx\right] = \frac{1}{2\Delta x}\left[h_1\Delta x + h_{12}\Delta x\right] \qquad \text{F-9}$$

$$h_3 = \frac{1}{3\Delta x}\left[\int_0^{x_2} h_x\,dx + \int_{x_2}^{x_3} h_x\,dx\right] = \frac{1}{3\Delta x}\left[2h_2\Delta x + h_{23}\Delta x\right] \qquad \text{F-10}$$

Hence

$$h_{12} = 2h_2 - h_1 \qquad \text{F-11}$$

$$h_{23} = 3h_3 - 2h_2 \qquad \text{F-12}$$

$$h_{34} = 4h_4 - 3h_3 \qquad \text{F-13}$$

In the present analysis, the copper plate was divided into six radial increments and axial increments as shown on Figure 17 for a low h study and Figure 18 for a high study. At the coordinates designating each unit of the network, numbers in circles indicate the equations which are applicable. Below this and to the right is noted the steady state temperature which would prevail if the heat transfer coefficient were constant over the entire heat transfer surface. To the left is noted the temperature which appears as a result of the iterative procedure, with the allowance for variation of the heat transfer coefficient. The details of the conditions of the analysis are as follows:

n = 12	r_o = 0.0625 in.	r_{10} = 0.8828 in.
D = 1/8 in.	r_2 = 0.1061 in.	r_{12} = 1.500 in.
L = 1/8 in.	r_4 = 0.1803 in.	Δx = 0.0312 in.
q = 280 Btu/hr	r_6 = 0.3061 in.	P = 1.698
$k_{(copper)}$ = 220 Btu/hr ft^2 ^oF/ft	r_8 = 0.5198 in.	N = 301.81

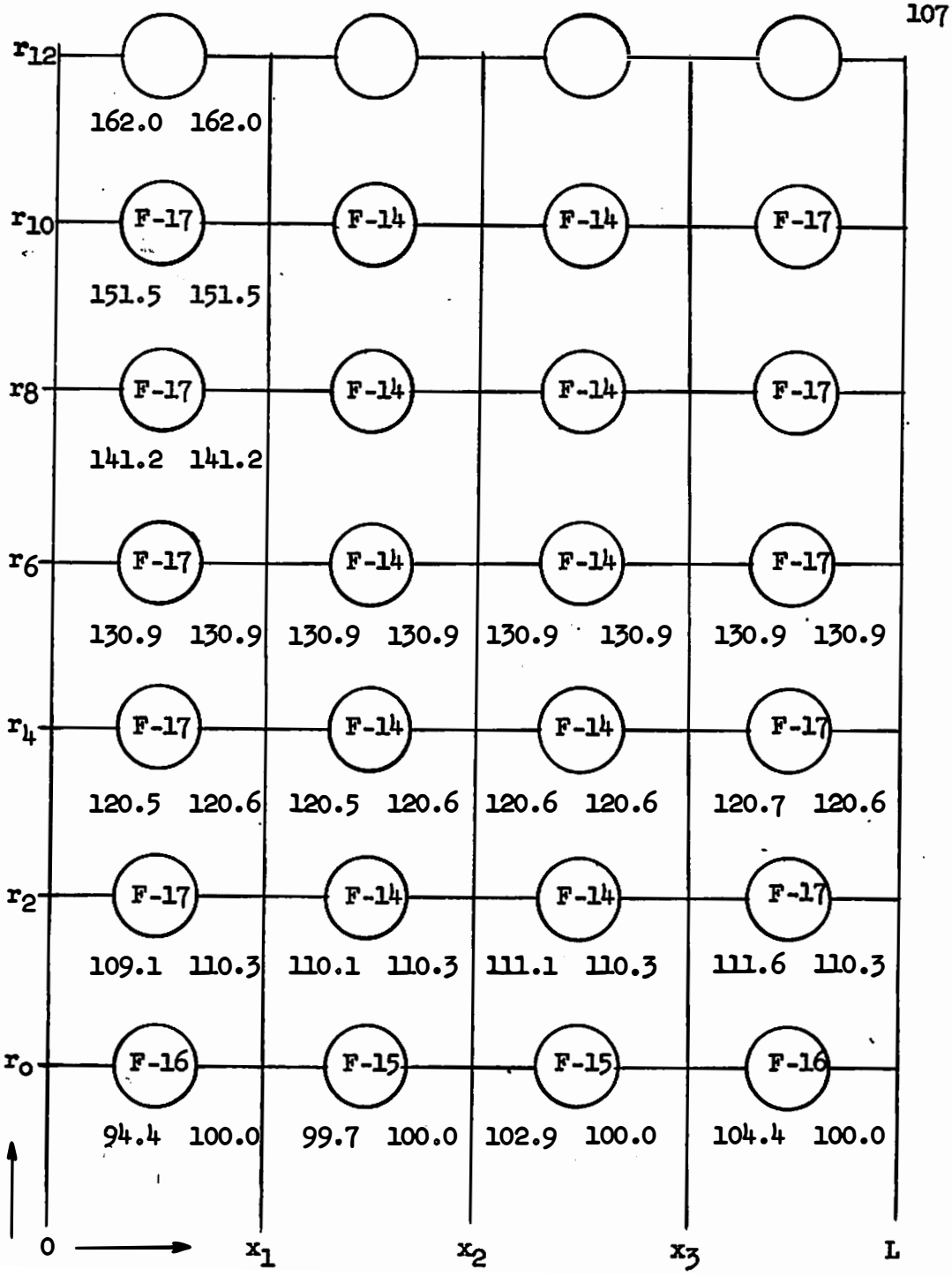

FIG. 17 TEMPERATURE DISTRIBUTION IN TEST SECTION
LOW h SYSTEM

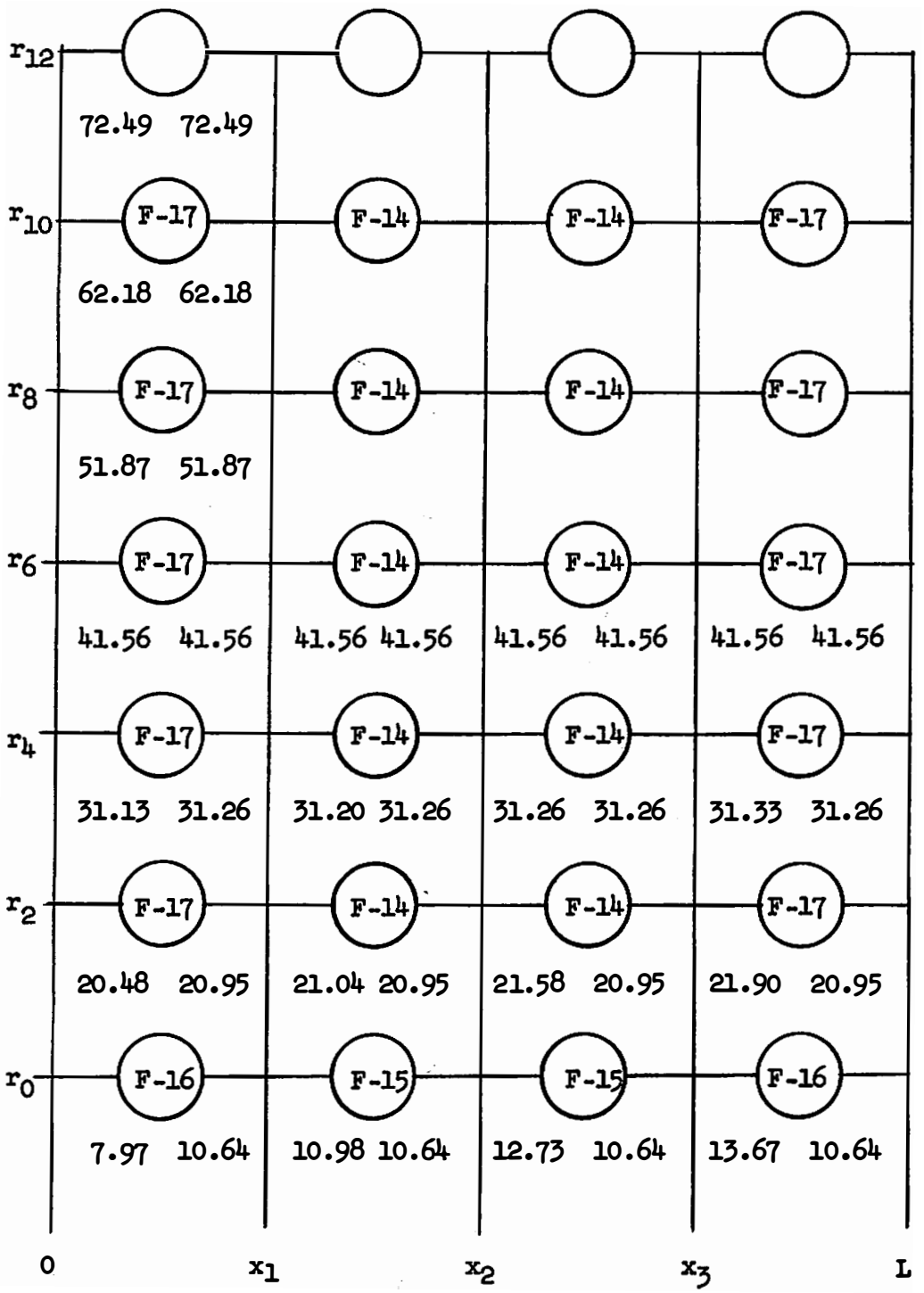

FIG. 18 TEMPERATURE DISTRIBUTION IN TEST SECTION
HIGH h SYSTEM

	low h	high h
h_{01}, Btu/hr. ft.^{2} $^\circ$F	15700	147600
h_{12}	7025	66020
h_{23}	5485	51560
h_{34}	4680	43980
h_{04}	8220	77290

Additional equations used in the analysis are listed below:

$$t_o = \frac{r_n^2(301.81)(t_1+t_3) + t_2 + t_4}{2(301.81 r_n^2+1)} \qquad \text{F-14}$$

$$t_o = \frac{0.742(t_1+t_3)+t_2}{2.484 + h(1.254\times10^{-5})} \qquad \text{F-15}$$

$$t_o = \frac{0.742 t_1 + t_2}{1.742 + h(1.254\times10^{-5})} \qquad \text{F-16}$$

$$t_o = \frac{r_n^2(301.81)t_1 + t_2 + t_4}{301.81 r_n^2 + 2} \qquad \text{F-17}$$

The results of the analysis of the wall temperature in the test section are summarized on Table X. Comparison is made with the temperatures which would prevail if the case were one of uniform heat flux.

The two examples, having average heat transfer coefficients of 8220 and 77290 Btu/hr. ft.^{2} $^\circ$F., serve to bracket the range of experimental measurements of heat transfer to mercury, from which coefficients from 10300 to 66300 were obtained. In the example with low heat transfer coefficient, the deviation of wall temperature from the uniform postulated value is found to be greatest in the first increment

TABLE X

WALL TEMPERATURE IN THE TEST SECTION

For low h System Increment	Postulated t, °F	Computed t, °F Iterative Process	Uniform Flux
1	100	94.4	52.4
2	100	99.7	117.1
3	100	102.9	149.9
4	100	104.4	175.7
For high h System Increment	**Postulated t, °F**	**Computed t, °F Iterative Process**	**Uniform Flux**
1	10.64	7.97	5.58
2	10.64	10.98	12.46
3	10.64	12.73	15.95
4	10.64	13.67	18.69

of length, averaging 5.6% of the difference between the heat transfer surface temperature and the mean mercury temperature. Average deviation over the entire heated length is about 3.3% of this temperature difference.

In the example with high heat transfer coefficient, the greatest average deviation from uniform temperature amounts to about 28.5% and it occurs in the last increment of heated length. The average deviation over the entire length is about 19%. As shown on Table X, the wall temperature distribution is intermediate between the postulated uniform temperature and that which would result in a case of uniform heat flux. Hence, at the operating conditions yielding high heat transfer coefficients, this particular system tends toward a case of uniform flux. In the analytical solutions for uniform velocity streams, it is found that predicted average Nusselt moduli for the uniform wall temperature cases are only about 70% as high as predictions for cases of uniform heat flux. Consequently, one would expect that the experimental data should be high compared with the uniform wall temperature solutions in regions of high coefficient. Clearly, this trend is exhibited by the data, but the major influence in making the data high at the high region of Peclet modulus is the contribution of the eddy conduction, as noted previously in the text.

APPENDIX G

ERROR ANALYSIS

In Chapter V, it was pointed out that the experimental values of heat transfer coefficients were computed from the equation

$$h = \frac{q}{A(t_w - t_m)} \qquad \text{G-1}$$

where the heat rate q was determined by the slope S of the experimentally determined temperature gradient in the test section, according to the following expression:

$$(t_r - t_w) = \frac{q}{2\pi k_c L} \ln \frac{r}{b} = S \ln \frac{r}{b} \qquad \text{G-2}$$

In Equation G-2, t_r is the temperature in the center plate at radius r, and t_w is the plate surface temperature at r = b; k_c is thermal conductivity of the plate and L is the plate thickness. Values of the surface temperature were obtained by extrapolating the measured temperature gradient to the radius r = b.

Experimental errors may be examined on the basis of the equations noted above (38), describing data from three different test sections. Here the heat transfer coefficient h is seen to be a function of heat rate q, surface temperature t_w, mean liquid temperature t_m and surface area A, all of which are determined from experimental measurements.

$$h = f(q, t_w, t_m, A) \qquad \text{G-3}$$

$$dh = \frac{\partial f}{\partial q} dq + \frac{\partial f}{\partial t_w} dt_w + \frac{\partial f}{\partial t_m} dt_m + \frac{\partial f}{\partial A} dA \qquad \text{G-4}$$

or

$$\Delta h = \frac{\partial f}{\partial q}\Delta q + \frac{\partial f}{\partial t_w}\Delta t_w + \frac{\partial f}{\partial t_m}\Delta t_m + \frac{\partial f}{\partial A}\Delta A \qquad \text{G-5}$$

From Equations G-1 and G-5, one gets

$$\frac{\Delta h}{h} = \frac{\Delta q}{q} - \frac{\Delta t_w - \Delta t_m}{t_w - t_m} - \frac{\Delta A}{A} \qquad \text{G-6}$$

In practice, $\frac{\Delta h}{h}$ may be expressed as the sum of absolute values of the other terms so as to obtain the maximum error.

Since $S = \frac{q}{2\pi k_c L}$, one may write

$$\frac{\Delta q}{q} = \frac{\Delta L}{L} + \frac{\Delta S}{S} \qquad \text{G-7}$$

Note that the $\frac{\Delta k_c}{k_c}$ term would be required in the estimate of accuracy, but it is not included in an estimate of precision. Since data from three different test sections are compared, the influence of physical dimensions and thermocouple locations must be involved in estimating the errors. The uncertainty in thermocouple location is about 0.002 inch. If r_2 = 1 1/4 in. and r_1 = 1/4 in., one may obtain the relation

$$\frac{\frac{\Delta r_2}{r_2} + \frac{\Delta r_1}{r_1}}{\ln \frac{r_2}{r_1}} = \frac{\frac{0.002}{1.25} + \frac{0.002}{0.25}}{\ln 5} = 0.009 \qquad \text{G-8}$$

Values of Δt_r and Δt_w may best be estimated by evaluating a set of temperature measurements by the method of least squares. Equation G-2 yields a linear plot of t_r with respect to $\ln \frac{r}{b}$, having an intercept t_w at r = b. Using data of Run 5 obtained in the mercury system, the least squares analysis is shown on Table XI. The average deviation is

TABLE XI

LEAST SQUARES ANALYSIS OF RADIAL TEMPERATURE DISTRIBUTION IN TEST SECTION

Run 5, Mercury System

	$x = \ln \frac{r}{b}$	y=t	x^2	xy	gx	y_c	$\lvert y-y_c \rvert$
1	1.3863	158.6	1.92183	219.87	28.32	158.81	0.2
2	1.3863	158.7		220.01			0.1
3	2.0794	173.6	4.32390	360.98	42.47	172.96	0.6
4	2.0794	173.2		360.15			0.2
5	2.6391	185.8	6.96485	490.34	53.90	184.39	1.4
6	2.6391	184.9		487.97			0.5
7	2.9957	191.0	8.97422	572.18	61.19	191.68	0.7
8	2.9957	191.7		574.28			0.0
	18.2010	1417.5	44.36960	3285.78			3.7

NOTE: Numbers in the first column designate the thermocouples in the test plate. The form of the equation assumed for the analysis is $y = y_o + gx$. Values of the constants determined by the analysis are $y_o = 130.49$ and $g = 20.524$. The average error is assumed to be the average of the absolute value of the deviation from the mean, about $0.4^{\circ}F$.

about 0.5 °F., and this will be considered as an appropriate value of Δt_r. Let $\Delta t_w = 2\ \Delta t_r$ or 1°F.

$$\frac{\Delta t_{r_2} + \Delta t_{r_1}}{t_{r_2} - t_{r_1}} = \frac{1}{25} = 0.04 \qquad \text{G-9}$$

Hence,

$$\frac{\Delta S}{S} = \frac{\Delta t_{r_2} + \Delta t_{r_1}}{t_{r_2} - t_{r_1}} + \frac{\frac{\Delta r_2}{r_2} + \frac{\Delta r_1}{r_1}}{\ln \frac{r_2}{r_1}} = 0.04 + 0.009 = 0.049 \qquad \text{G-10}$$

Letting L = 0.001 in., Equation G-7 may now be evaluated.

$$\frac{\Delta q}{q} = \frac{\Delta L}{L} + \frac{\Delta S}{S} = \frac{0.001}{1/16} + 0.049 = 0.065 \qquad \text{G-11}$$

The error in heat transfer area is obtained by considering possible errors in hole diameter as well as errors in plate thickness. That is,

$$A = 2\pi b L \qquad \text{G-12}$$

$$\frac{\Delta A}{A} = \frac{\Delta b}{b} + \frac{\Delta L}{L} \qquad \text{G-13}$$

The uncertainty in b and L is about 0.001 in., hence

$$\frac{\Delta A}{A} = \frac{0.001}{1/32} + \frac{0.001}{1/16} = 0.048 \qquad \text{G-14}$$

the change of mean fluid temperature t_m within the test section is of the order of 4 or 5 °F for the mercury runs. The error in t_m is arbitrarily taken as 1 °F. Summing up the errors for heat transfer coefficient in the three test sections, according to Equation G-6, one gets

$$\frac{\Delta h}{h} = \frac{\Delta q}{q} + \frac{\Delta t_w + \Delta t_m}{t_w - t_m} + \frac{\Delta A}{A} = 0.065 + \frac{1+1}{50} + 0.048 = 0.153 \qquad \text{G-15}$$

This error is reflected in the Nusselt modulus in the following manner:

$$\frac{\Delta(Nu)}{Nu} = \frac{\Delta h}{h} + \frac{\Delta D}{D} = 0.153 + \frac{0.002}{1/16} = 0.185 \qquad \text{G-16}$$

On this basis, the errors in Nusselt modulus for the three test sections may amount to 18.5%. Since these data are plotted against $Pe\,\frac{D}{L}$, it is of interest to examine errors in this term.

$$Pe\,\frac{D}{L} = \frac{4Wc}{\pi k L} \qquad \text{G-17}$$

$$\frac{\Delta(Pe\,\frac{D}{L})}{Pe\,\frac{D}{L}} = \frac{\Delta W}{W} + \frac{\Delta L}{L} \qquad \text{G-18}$$

In practice, W was computed by measuring the time required for a certain volume of mercury to flow into the catch tank. The error in mass of mercury required to occupy the measured volume is set at 1% on the basis of the variation in actual measurements. The shortest time increment required for filling the catch tank was 5.0 seconds on a timer which measured to 0.1 seconds. Hence

$$\frac{\Delta W}{W} = \frac{\Delta M}{M} + \frac{\Delta \theta}{\theta} = 0.01 + \frac{0.1}{5} = 0.03 \qquad \text{G-19}$$

and

$$\frac{\Delta(Pe\,\frac{D}{L})}{Pe\,\frac{D}{L}} = 0.03 + 0.016 = 0.046 \qquad \text{G-20}$$

In the region of the present experimental data, an error along the abscissa, $Pe\,\frac{D}{L}$, would show itself as about half as much error along the ordinate, Nu. One can account in this way for a precision of about

± 21.0% for the data of the three test sections when plotted as Nu vs. $Pe \frac{D}{L}$. The accuracy of the data is of the same order as the precision plus the additional uncertainty of the physical properties of the fluid. The data of Hall (15) and Gehlhoff and Neumeier (12) for the thermal conductivity of mercury differ by about 35% in the temperature range of interest.

APPENDIX H

NOMENCLATURE

Moduli

Nu	Nusselt	$\frac{hD}{k}$
Pe	Peclet	$\frac{DU}{\alpha}$
Pr	Prandtl	$\frac{c\mu}{k}$
Re	Reynolds	$\frac{DU\rho}{\mu}$

Capital letters

A	heat transfer area, ft^2
B	constant in power law expression, ft./hr.
D	channel diameter or equivalent diameter, ft.
L	channel length, ft.
M,N,P,Q,R	arbitrary functions defined in Appendix E
M	mass, lb.
R	interfacial electrical resistance, ohm
S	slope, $\frac{q}{2\pi kL}$, ^{o}F
U	average fluid velocity, lb./hr.
W	flow rate, lb./hr.

Lower case letters

a	thermal diffusivity, ft.^{2}/hr., or radius as used in Appendix E, ft.
b	radius or half distance between plates, ft.
c	heat capacity, Btu/lb. ^oF.
f	functional notation as used in Appendix G
g	arbitrary constant, Appendix G
h	heat transfer coefficient, Btu/hr.ft.^{2} ^oF.
k	thermal conductivity, Btu/hr. ft.^{2} ^oF/ft.
m	exponent in power law expression
m_n	exponent in parabolic flow solution, Appendix A
q	heat rate, Btu/hr.
r	radius, ft.
t	temperature, ^oF.
u	local velocity, ft./hr.
x,y,z	distance coordinates, ft.

Greek letters

α_n	positive roots of $J_o(\alpha) = 0$
β_n	defined as $(2n-1)\pi$
γ_n	roots used in parabolic flow solution, Appendix A
ϵ_H	eddy diffusivity of heat, ft.^{2}/hr.
θ	time, hr.
μ	viscosity, lb./ft. hr.
ρ	density, lb./ft.^{3}; or resistivity in ohm cm

Φ	angular displacement in cylindrical coordinates
Ψ	see Appendix A
Ω	see Appendix B

Subscripts

c	computed value, or denotes property of copper plate
f	denotes property of fluid
L	average value over length L
m	denotes mean fluid property
o	observed value, or initial fluid condition, or condition at origin of network unit
r	denotes condition at radius r
w	denotes condition at channel wall
x	local value, or property of unknown substance

Abbreviations

b.p.	boiling point
psi	pressure in lb./in.^{2}
ln	natural logarithm